Journal of Marine Systems 189 (2019) 22–35

Contents lists available at ScienceDirect

Journal of Marine Systems

journal homepage: www.elsevier.com/locate/jmarsys

Nutrient and carbon dynamics under the water mass seasonality on the continental shelf at the South Brazil Bight

Luís Henrique Bordin[a,*], Eunice da C. Machado[b], Melissa Carvalho[c], Andrea S. Freire[c], Alessandra L.D.O. Fonseca[d]

[a] Programa de Pós-Graduação em Oceanografia, Universidade Federal de Santa Catarina, Florianópolis 88040-900, SC, Brazil
[b] Instituto Oceanográfico, Universidade Federal do Rio Grande, Rio Grande 96203-900, RS, Brazil
[c] Departamento de Ecologia e Zoologia, Universidade Federal de Santa Catarina, Florianópolis 88040-900, SC, Brazil
[d] Coordenadoria Especial de Oceanografia, Universidade Federal de Santa Catarina, Florianópolis 88040-900, SC, Brazil

ARTICLE INFO

Keywords:
Nutrient dynamics
Particulate organic carbon
Regeneration processes
South Atlantic Ocean

ABSTRACT

The enrichment of the euphotic zone and the production of organic matter (OM) are induced by wind-driven processes that change the water mass distribution in the central inner and mid continental shelf of Santa Catarina State (27°18′–27°37′S), South Brazil Bight (23–28.5°S). During austral summer, the Ekman transport by north-eastern winds is balanced by onshore bottom intrusions of the nutrient-rich South Atlantic Central Water (SACW), while during austral winter, the Plata Plume Water (PPW) reaches the region, which is pushed northward by south-eastern winds. Between 2014 and 2016, six oceanographic campaigns were conducted at the isobaths of 30 and 50 m, one in the early fall of 2014, others in the summers of 2015 and 2016, and in each winter of the stated years. The aim was to investigate the spatio-temporal variability of nutrients (nitrate + nitrite, ammonium, phosphate and silicate), and composition of the particulate organic matter (POM), i.e. particulate organic carbon and nitrogen, in relation to the water masses dynamics. In summer of 2015 and 2016, the SACW reached all over the bottom layers of the studied area, while in 2014, it only reached the outer stations. The SACW intrusion was reflected by relatively high phosphate (0.61 ± 0.29 μM), silicate (9.51 ± 4.34 μM), and notably high nitrate (4.21 ± 2.83 μM) concentrations. The POM composition revealed the deep chlorophyll-*a* maximum at intermediate and bottom layers, indicating new primary production associated with the nutrient-rich SACW. The denitrification was identified in bottom water by nitrogen loss (up to 9.66 μM) associated with the low dissolved oxygen saturation (DO%) (53.07 ± 7.8%). In winter, the PPW reached the region in the surface, especially in 2015 and 2016, with high silicate concentrations (8.36 ± 2.46 μM). Nitrate (1.69 ± 0.92 μM) and phosphate (0.46 ± 0.23 μM) were mainly related to regeneration processes in the bottom layers associated with low DO% (78.25 ± 7.55%). In summer, the SACW presented higher potential for biological production against Subtropical Shelf Water (STSW), while in winter, the STSW was higher than the PPW. Besides the new nutrient supply associated with wind-driven water mass dynamics, the nutrients regeneration contributed to the food chain structure via a regenerated primary production.

1. Introduction

Wind-driven processes, such as onshore deep intrusions of cold and nutrient-rich oceanic water masses as well as continental drainage by river runoff are important processes that fertilise and influence the continental shelf ecosystems worldwide, enhancing primary production and associated organic matter (OM). However, despite the supply of allochthonous nutrients by these sources, regeneration processes also play an important role in supporting the maintenance of primary production along the year (Mann and Lazier, 2006; Falkowski and Raven, 2007; Valiela, 2015).

The hydrodynamics and the biogeochemical processes, such as OM production and regeneration affect the nutritional conditions of water mass. The potential for biological production can be categorized in classes of trophic status, e.g. oligotrophic (nutrient poor – low productivity) and eutrophic (nutrient rich – high productivity) (Vollenweider et al., 1998; Cloern et al., 2014). The trophic index TRIX is a tool used to characterize the trophic state and to evaluate the water quality in coastal marine waters. The index equation is based on chlorophyll-*a* (Chl-*a*), nutrients and oxygen saturation, scaled from 0 to

* Corresponding author.
E-mail address: graoceano@gmail.com (L.H. Bordin).

https://doi.org/10.1016/j.jmarsys.2018.09.006
Received 14 June 2018; Received in revised form 6 September 2018; Accepted 19 September 2018
Available online 21 September 2018
0924-7963/

10, covers a wide range of trophic conditions from oligotrophy to eutrophy (Vollenweider et al., 1998).

The particulate organic carbon (POC) production, consumption and exportation on marine ecosystems are processes that impact the carbon biogeochemistry dynamics (Giering et al., 2014). The nature, distribution and variability of particulate organic matter (POM) in the oceans are considered key factors for the understanding of the carbon biogeochemical cycle (Sabine et al., 2004; Honjo et al., 2008). The establishment of POM relations with hydrochemical and Chl-*a* dynamics are essential to understand the functioning of the coastal systems, because the production and oxidation of the OM regulate the fluxes of matter and energy thorough the food chains and the air-sea CO_2 exchange. The POM nature and quality are usually evaluated by the relation between POC and particulate organic nitrogen (PON) (C:N elemental ratios) and by the POC and Chl-*a* (POC:Chl-*a* ratios) (Savoye et al., 2003; Liénart et al., 2016).

Studies on POM dynamics are scarce in the continental shelf of the South Brazil Bight (SBB) (23–28.5°S) (Bergo et al., 2017; Coelho-Souza et al., 2017), and even more on the coast of the Santa Catarina State (SC) (Brandini et al., 2014; Gérikas-Ribeiro et al., 2016; Fontes et al., 2018), Brazil's one of the most fishery productive region (Wainer and Taschetto, 2006). The state of SC is in the southernmost portion of the SBB—a transitional zone between the subtropical and temperate regions of the western boundary current system (Loder et al., 1998)—mostly influenced by wind-driven processes (Castro et al., 2006) that affect the shelf ecosystems productivity and fisheries (Brandini et al., 2018; Fontes et al., 2018).

During summer, northeast winds promote the Ekman transport of surface waters offshore, which is balanced by onshore bottom intrusions of the nutrient-rich South Atlantic Central Water (SACW) (Castro and Miranda, 1998; Campos et al., 2000). The solar heating at the surface, and the intrusion of cold SACW in the bottom create a seasonal thermocline (Matsuura, 1986; Castro et al., 2006), which also enhance the depth of the euphotic zone (Brandini et al., 2014). The winter period shows strong wind instability with the frequent passage of south and southeast cold fronts (Castro et al., 2006). The southern winds cause a northward displacement of a nutrient-rich (Braga et al., 2008) and low salinity tongue formed by the La Plata River and the Patos-Mirim Lagoon discharges, known as Plata Plume Water (PPW) (Piola et al., 2000; Möller et al., 2008). Depending on the intensity and persistence of the south-eastern winds, the PPW reaches below 28°S (Piola et al., 2005). Due to the higher content of PPW terrigenous material, the euphotic zone becomes shallower (Nagai et al., 2014). On the other hand, the more intense winds and tides prevent the formation of physical stratification by intensively mixing the water column, mostly at the mid-shelf (Castro et al., 2006; Freire et al., 2017). The area is also under relative influence of the Tijucas River Plume Water (TPW) and Florianópolis North Bay Channel Water (NBW), mostly during intense rainfall periods (Freire et al., 2017).

The SACW and PPW are important sources of nutrients for SBB coastal ecosystems, enhancing the local primary production, and hence, the entire biological production. The OM oxidation is also a regular source of regenerated nutrients, maintaining to a lesser extent the annual rates of primary production. Therefore, this study was carried out to: (i) investigate the nutrients and POM dynamics according to the water mass seasonality; (ii) assess the POM nature and origin using the POC:Chl-*a* and elemental C:N ratios; and (iii) infer about the ecosystem potential for biological production by means of the TRIX trophic index.

2. Material and methods

2.1. Field work

Within the scope of the “Environmental Monitoring of the Arvoredo Marine Biological Reserve and Surroundings” (MAArE, 2017) project, six oceanographic campaigns were conducted between 2014 and 2016: in the early fall of 2014 (representative of summer), in the summers of 2015 and 2016, and in each winter of the stated years. Six stations were sampled in each campaign at the mid- and inner-shelf (width and depth vary at seasonal scale according to the bottom thermal front and surface haline front) (Castro et al., 2006): three close to the 30 m isobath, and other three to the 50 m isobath (Fig. 1). At each station, samples were collected in three depths of the water column: surface, intermediate and bottom. The intermediate depth was defined by the maximum of fluorescence depth or by the mixed layer depth.

Salinity, temperature and depth were obtained by a CTD (SBE 19plus V2 SeaCATplus Profiler CTD) equipped with dissolved oxygen (SBE 43) and Chl-*a* fluorescence (WET Labs ECO-FLrt) sensors. The

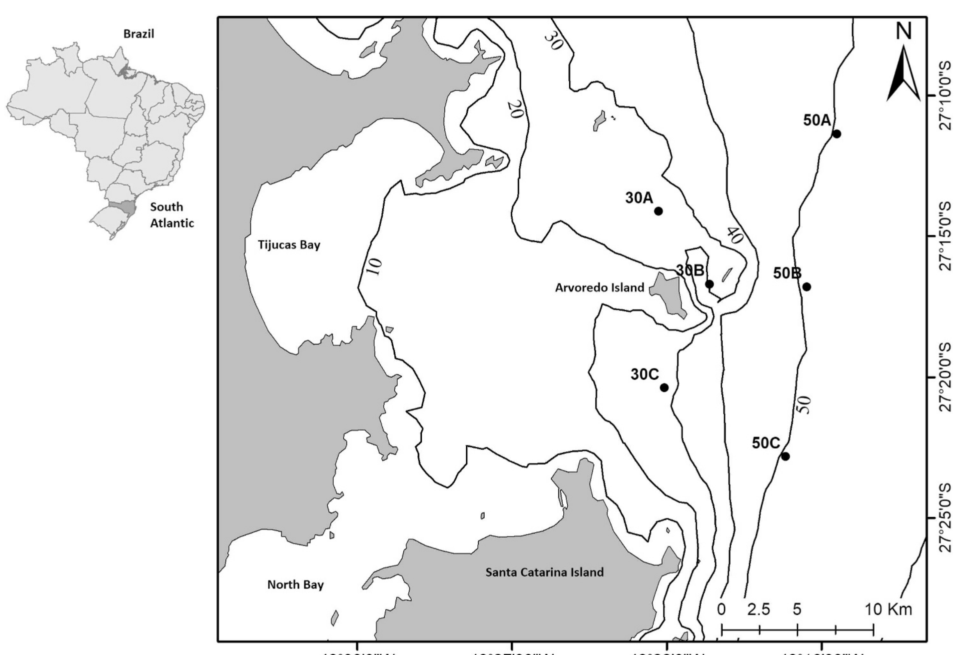

Fig. 1. Study area on the inner and mid continental shelf of Santa Catarina State (upper left map, dark gray), South Brazil Bight, with sampling stations at the 30 m isobath (30A, 30B and 30C) and at the 50 m isobath (50A, 50B and 50C).

water samples, used to determine the concentrations of dissolved inorganic nutrients (nitrate + nitrite, ammonium, phosphate and silicate), POM i.e., POC and PON, were collected using a Van Dorn bottle. Samples were conditioned in 5 L thermic bottles and filtered immediately at the vessel. The euphotic zone depth (Zeu) data was determined from Secchi disk readings (Zeu = depth of disk disappearance multiplied by 2.7) (Cole and Weihe, 2015) and concentrations of Chl-*a* (SCOR-UNESCO, 1966), were provided by the MAArE project. The wind intensity and direction data of fifteen days prior to each campaign were downloaded for station No. 83897 (São José, about 30 km south from the area) of Banco de Dados Meteorológicos para Ensino e Pesquisa (BDMEP) of Instituto Nacional de Meteorologia (INMET - Instituto Nacional de Meteorologia, 2017).

2.2. Samples processing

Concentrations of dissolved inorganic nutrients (μM) were determined using Whatmann GF/F filters (0.7 μm of porosity) under controlled pressure and were preserved frozen (−8 °C) until sample analysis (Grasshoff et al., 1983). The water samples were thawed at laboratory temperature for the colorimetric analysis under a spectrophotometer (Hitachi U-2900 provided with siper). Nitrogen and phosphate ratios (N:P) were calculated by dividing dissolved inorganic nitrogen (sum of nitrate, nitrite and ammonium concentrations - DIN) by phosphate concentrations (Libes, 2009). The POC and PON were concentrated using a fiberglass filter with 25 mm of diameter, and their analysis followed Wallner-Kersanach and Machado (2010). The filters were previously calcined, decarbonated, dried, weighed, and then analysed in a Perkin Elmer CHNS/O 2400 Series. The POC and PON data were available only for 2016.

2.3. Data analysis

Temperature and Salinity diagrams with oxygen saturation (DO%), nitrate, ammonium, phosphate, silicate and TRIX were produced in the Ocean Data View software (Schlitzer, 2018) to analyse the variation of these variables in relation to water masses. The boundaries of each water mass were determined according to the termohaline intervals described by Möller et al. (2008) (Table 1).

To verify the POM origin and composition, we calculated the POC:Chl-*a* ratio by dividing POC ($\mu g{\cdot}L^{-1}$) by Chl-*a* ($\mu g{\cdot}L^{-1}$), and the C:N elemental ratios by transforming POC and PON ($\mu g{\cdot}L^{-1}$) into molar units, and then, dividing C unit by N unit (Savoye et al., 2003; Liénart et al., 2016). The ratios discriminate living phytoplankton (POC:Chl-*a* ≤ 100) or phytoplankton-dominated POM (POC:Chl-*a* < 200) from detrital or degraded material (POC:Chl-*a* > 200), and heterotrophs (zooplankton and bacteria) (C:N 3–6) from phytoplankton (C:N 6–10) and terrestrial detritus (C:N > 12).

For the summer campaigns, we also verified the nitrogen denitrification processes by means of two simple stoichiometric methods that compare the expected and the observed nitrate concentrations in the water. The first method (Libes, 2009) consists of multiplying the phosphate observed in situ by the N:P ratio to determine the expected nitrate concentration. The phytoplankton OM is oxidized and the remineralized nutrients return to the water column in the same N:P proportion (Redfield et al., 1963). Once the phosphorus is more conservative than the nitrogen because of the lack of a gaseous phase (Gordon et al., 1996), the Redfield N:P ratio (16:1) or the mean N:P ratio of a given water mass can be used to calculate which would be the expected nitrate values in the water. If this observed concentration of nitrate is lower than the expected one, a loss might have occurred because of denitrification (Libes, 2009). We used 13:1 as the mean SACW N:P ratio accordingly to Gaeta and Brandini (2006).

The second method (Braga and Muller, 1998) considers the stoichiometry of the oxygen consumed in OM oxidation. The method estimates the nitrogen regeneration during the SACW onshore bottom intrusion by the oxygen consumed along the cross-shelf water mass displacement, i.e. by the difference between oxygen concentrations at the beginning of the SACW intrusion and its value in the mid- and inner-shelf. This difference corresponds to OM oxidation. The 208.6 μM value registered at 300 m depth (Braga and Muller, 1998) was considered the SACW initial oxygen concentration. Since all ammonium resulting from oxidation of OM is converted into nitrate by nitrification, we estimated the expected nitrate concentration dividing the dissolved oxygen (DO) variation by 10.3 μM. The value of 10.3 μM is the stoichiometric relation of DO consumed to oxide 1 μM of nitrate (Rios, 1992; Alvarez-Salgado, 1993).

The regeneration methods were applied only to summer conditions of the SACW below the Zeu. We could not determine the PPW ratio (Libes's method), once there is phytoplankton assimilation, phosphate flocculation and adsorption throughout the northward PPW displacement (Brandini, 1990; Braga et al., 2008). Likewise, DO stoichiometry (Braga and Muller's method) was inappropriate since the PPW is subjected to phytoplankton activity and air-sea oxygen exchanges.

We also calculated the trophic index TRIX (Vollenweider et al., 1998) to classify the potential for biological production of the water masses. The index was calculated by Eq. (1), as follows:

$$\mathrm{TRIX} = [\log(\mathrm{Chl} - a.\ \mathrm{aD\%O.\ N.\ P}) - (\mathrm{a})]/\mathrm{b} \tag{1}$$

where:

Chl-*a* [$mg\,m^{-3}$] = the effect of the nutritional conditions for the phytoplankton growth;

aD%O = dissolved oxygen as an absolute deviation of saturation [%], as a way of measuring the balance between production and respiration;

N = dissolved inorganic nitrogen as N-(NO_3^{-2} + NO_2^{-3} + NH_4^{+}) [μg/L];

P = dissolved inorganic phosphorus as P-PO_4^{-3} [μg/L].

Parameters a and b are scale coefficients used to fix the lower limit value of the index and the extension of the trophic scale from 0 to 10 TRIX units. In this study, the following were determined: a = −0.8 and b = 0.78. The classes were: ultra-oligotrophic (0–2), oligotrophic (2,01–4), mesotrophic (4,01–6), eutrophic (6,01–8) and hyper-eutrophic (8,01–10) (Vollenweider et al., 1998).

The analyses were performed with all the correspondent data from the three years (2014, 2015 and 2016). The mean (± standard deviation) values characterizing the properties of each water mass were calculated. Kruskal Wallis one-way analysis of variance (KW) (Dodge, 2008) were performed to test the differences ($p < 0.05$) of the parameters (temperature, salinity, nitrate, ammonium, DIN, percentage of nitrate about total DIN (NO_3^-%), N:P ratio, phosphate, silicate, DO, DO %, TRIX, POC, PON, POC:Chl-*a* and C:N ratios) between factors water masses and amongst factors water column layers. The water masses analysed in summer were: SACW (n = 18), STSW (n = 36); and in winter: PPW (n = 32), STSW (n = 22). The layers corresponded to surface, intermediate and bottom (n = 18 each season, n = 54 total). POC, PON, POC:Chl-*a* and C:N ratios were only analysed for 2016, by water mass (summer: SACW n = 5, STSW n = 11; and winter: PPW n = 18, STSW absent) and by layer (surface, intermediate and bottom: n = 6 each, n = 18 total). The principal component analysis (PCA) (Oksanen et al., 2018) was performed to verify the association between

Table 1
Thermohaline intervals used to characterize water masses STSW (Subtropical Shelf Water), SACW (South Atlantic Central Water) and PPW (Plata Plume Water) according Möller et al. (2008).

Water mass	Summer	Winter
STSW	T > 18.5 °C, 35.3 < S < 36	T > 14 °C, 33.5 < S < 35.3
	T > 21 °C, 33.5 < S ≤ 35.3	T > 18.5 °C, 35.2 ≤ S < 36
SACW	T ≤ 18.5 °C, S ≥ 35.3	T ≤ 18.5 °C, S ≥ 35.3
PPW	T > 10 °C, S ≤ 33.5	T > 10 °C, S ≤ 33.5

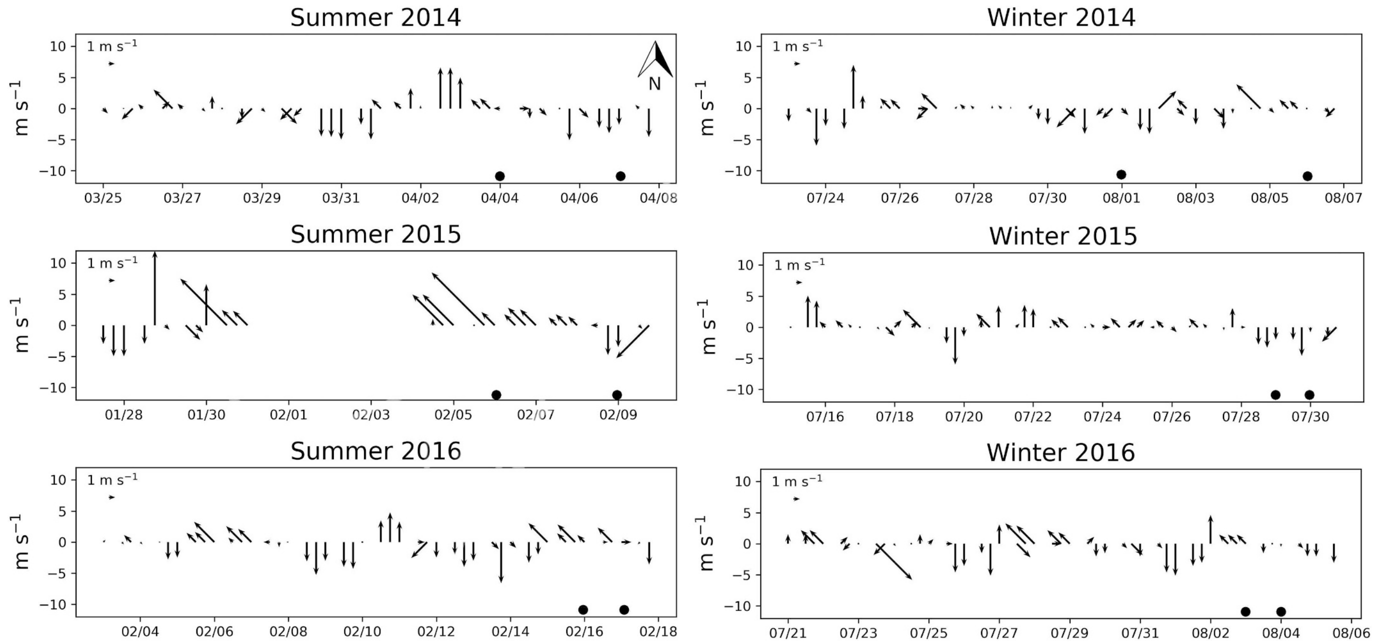

Fig. 2. The wind direction and intensity in m·s^{-1} (represented by vector length, legend on the upper left-hand side) fifteen days (x axis) prior to summer and winter sampling campaigns (2014, 2015 and 2016). The sampling dates are indicated by black dots on the x axis. Data from INMET station No. 83897.

the parameters: temperature, salinity, nitrate, phosphate, silicate, DO% and TRIX in each season (n = 54). Some TS pairs (2014 n = 1; 2015 n = 3; 2016 n = 1) were in the boundary of Tropical Water (TW) termohaline index. We considered these TS pairs as SACW (2014 and 2015, n = 4) because of the low temperature (< 20 °C) and its position at the intermediate and bottom layer; STSW (2016, n = 1) because of the high temperature (~24 °C), low salinity (~36) and its vicinity of the coast (Miranda, 1982). The TS pairs according Miranda (1982): TW (T > 20 °C; S > 36.4) and SACW (10° < T < 20 °C; 35 < S < 36.4). All statistical analyses were performed in the R software (R Core Team, 2018).

3. Results

3.1. Hydrography

During summer campaigns, wind direction was mainly from the north except during the summer of 2015, when intense south-easterly winds dominated reaching up to 12 m·s^{-1}. On the other hand, the winter was characterized by highly variable wind speed and direction with more intense winds from south and southeast (Fig. 2).

During summer, the STSW dominated from surface to 15.2 ± 5.76 m depth throughout the area. At deeper layers (35.75 ± 10.8 m) the SACW was registered, transported onshore by bottom intrusions caused by upwelling-favourable northerly winds (on the second sampling day in 2014 and 2015; in 2016 the wind was from north between 2016-02-11 and 2016-02-15, but rotated to the southeast one day prior to the first sampling day. Sampling dates for each campaign are shown in the Fig. 2). The water temperature varied from < 17 °C in bottom layers to > 27 °C at the surface. In 2016, there was a strong physical stratification at the 50 m isobath, with the thermal gradient reaching up to 10 °C because of the cold SACW at deeper waters. In 2014, the water was slightly homogeneous and the SACW was limited to the 50 m isobaths. In all summer campaigns, salinity ranged from < 34 at the surface to > 36 at the bottom. In 2014, the haline vertical amplitude was higher at the 50 m isobath, while in 2015 and 2016 the amplitude was higher (up to 2.64) at the 30 m isobath. The TW was identified punctually in the intermediate layer in 2015 and 2016, indicating its mixture with the other water masses.

The winter was characterized by the presence of the PPW at the surface, while the STSW was limited to bottom layers. The interannual variability was evident and both the thermal and the haline vertical gradients increased from 30 to 50 m isobaths. In 2014, the area was dominated by the STSW, presenting a homogeneous water column, with salinity ≥ and temperature > 18 °C. In 2015, the STSW was restricted to the intermediate and bottom layers with the surface dominated by the PPW with salinity < 34. In 2016, the region was dominated by the PPW, with salinity < 33.5 and temperature < 18 °C, along with the most homogeneous water column of all winter campaigns. Vertical profiles of temperature and salinity are plotted in the Fig. 10 (Appendix A) for each oceanographic campaign.

Overall, the Zeu (Table 2) was deeper during summer periods, reaching at least up to the intermediate layer in most cases, and the bottom at the 30 m isobath in 2015 (stations 30B and 30C) and 2016 (30A). During winter, the Zeu was shallower, reaching no further than the intermediate layer in 2014 and 2015, restricted to the upper layer in 2016. The mean Zeu depths of each oceanographic campaign are plotted in the Fig. 10 (Appendix A).

3.2. Hydrochemical properties and particulate organic matter

3.2.1. Austral summer

The vertical profile of hydrochemical variables in summer was mostly associated with the water masses distribution, which can be clearly observed by the data and variables grouping on the PCA mostly

Table 2
Average and standard deviation values of euphotic zone depth (m) for each oceanographic campaign performed in 2014, 2015 and 2016 on the inner and mid continental shelf of Santa Catarina State, South Brazil Bight, during austral summer and winter.
Data: MAArE (2017).

Isobath (m)		2014	2015	2016
Summer	30	13.68 ± 3.47	36.14 ± 20.5	30.38 ± 3.57
	50	25.33 ± 10.46	33.52 ± 2.53	38.92 ± 9.83
Winter	30	12.78 ± 2.18	21.15 ± 5.82	11.02 ± 2.16
	50	15.48 ± 7.76	21.15 ± 8.13	12.33 ± 5.70

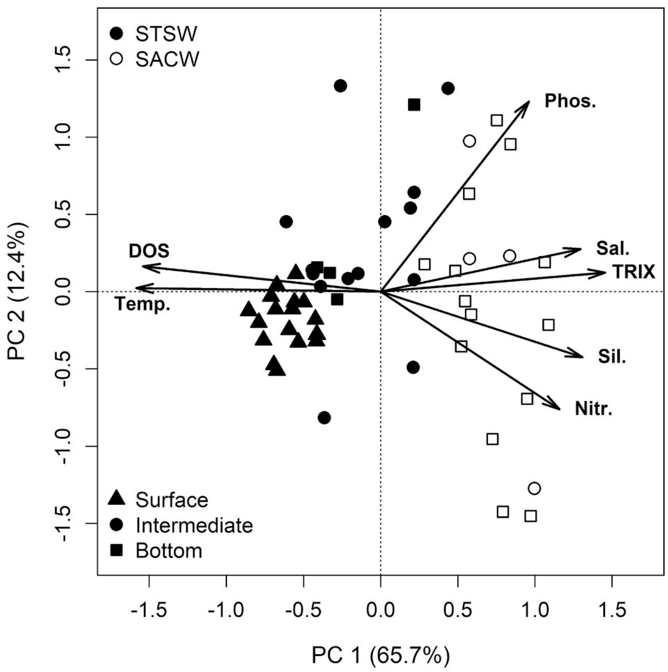

Fig. 3. Principal component analysis of the variables, namely, temperature (Temp.), salinity (Sal.), oxygen saturation (DOS), nitrate (Nitr.), Phosphate (Phos.), silicate (Sil.) and TRIX for the austral summer campaigns (2014, 2015 and 2016) on the inner and mid continental shelf of Santa Catarina State, South Brasil Bight. The water masses Subtropical Shelf Water (STSW – black) and South Atlantic Central Water (SACW – white) legend is on the upper left hand side; the water column layers (surface, intermediate and bottom) legend is on the bottom left hand side.

related to the principal component 1 (65.7% of data variance explanation) (Fig. 3). Nitrate, DIN, NO_3^-%, phosphate, silicate and TRIX increased (KW test: $p < 0.05$) from the surface, in the STSW, towards the bottom, in the colder and saltier SACW (Table 3), also indicated by the PCA negative correlation of temperature in relation to the nitrate, phosphate, silicate and TRIX (Fig. 3). The positive (negative) PCA correlation of temperature (salinity) in relation to the DO% revealed that DO% followed an inverse pattern than those variables cited above (Fig. 3).

Ammonium and N:P ratios did not show significant differences (KW test: $p > 0.05$) neither between the water masses nor amongst the water column layers. Mean and KW results are presented for each water mass and water column layer in Table 3. The values of each sample for the variables, namely, nitrate, ammonium, phosphate, silicate, DO% and TRIX in relation to water masses are shown in the TS diagrams (Fig. 4). Vertical profiles of DO are shown in the Fig. 10 (Appendix A) for each oceanographic campaign. SACW was considered mostly as eutrophic and STSW as mesotrophic by the TRIX mean water mass (Table 3).

In most cases, the negative values in the estimation of nitrogen regeneration for the summer in the SACW below the Zeu indicated a nitrogen loss according to Libes' (Libes, 2009) and Braga and Muller's (Braga and Muller, 1998) methods in most of the cases (Table 4). Though some differences were observed in the regenerated nitrogen values between the two methods, the means were similar (-5.21 ± 3.56 Libes, 2009; -4.63 ± 2.95 Braga and Muller, 1998). During 2016, the nitrogen loss occurred in more stations because of the SACW approximation towards the coast up to the 30 m isobath, below the Zeu (Fig. 10c - Appendix A).

During the summer of 2016, the POC and PON did not show significant differences between the water masses (KW test: H = 0.1 for POC; H = 0.21 for PON) and amongst the water column layers (KW test: H = 3.79 for POC; H = 3.03 for PON). The POC concentrations in general ranged between 300 and 650 $\mu g \cdot L^{-1}$; PON between 30 and 110 $\mu g \cdot L^{-1}$ (Fig. 5a and b respectively). Similarly, POC:Chl-*a* and C:N ratios did not show significant differences between water masses (KW test: H = 4.36 for POC:Chl-*a*; H = 2.85 for C:N) and water column layers (KW test: H = 3.86 for POC:Chl-*a*; H = 0.56 for C:N). POC:Chl-*a* ratios were mainly < 100 in SACW (86.46 ± 71.58) and < 200 in STSW (150.85 ± 87.78) (Fig. 5c). The C:N ratios ranged from 6 to 10 with mean values of 8.2 ± 3.23 for the SACW and 9.08 ± 2.45 for the STSW, with few values out of this range (Fig. 5d).

3.2.2. Austral winter

The PCA demonstrated that 69.2% of the data variance was explained by the first and second principal components (Fig. 6). The negative correlation of temperature and salinity in relation to the silicate and DO% as well as the data grouping by water mass (Fig. 6) shows that silicate and DO% were higher (KW test: $p < 0.05$) in the colder and fresher PPW than in the STSW, whereas the nitrate, phosphate and TRIX were higher in the STSW than in the PPW. Ammonium did not show significant differences between the water masses (KW test: $p > 0.05$). Regarding the vertical profile, nitrate, phosphate and TRIX increased (KW test: $p < 0.05$) towards the bottom, whereas DO and DO% decreased. Silicate and ammonium did not show significant differences between the water column layers (KW test: $p > 0.05$).

Table 3
Mean (± standard deviation) values for all variables and results of Kruskal Wallis one-way analysis of variance (p: p-value/H: chi-squared) for the austral summer campaigns (2014, 2015 and 2016) on the inner and mid continental shelf of Santa Catarina State, South Brazil Bight. KW tested differences between factors water mass (SACW - South Atlantic Central Water; STSW - Subtropical Shelf Water) and amongst factors water column layer (surface, intermediate and bottom).

	STSW	SACW	KW (p/H)	Surface	Intermediate	Bottom	KW (p/H)
Temperature (°C)	24.76 ± 2.01	17.96 ± 0.85	***/34.55	26.15 ± 0.92	22.27 ± 2.79	19.09 ± 2.58	***/37.08
Salinity	35.06 ± 0.65	35.97 ± 0.20	***/29.26	34.67 ± 0.59	35.56 ± 0.53	35.87 ± 0.26	***/31.67
Nitrate [μM]	1.15 ± 1.45	4.21 ± 2.83	***/12.33	0.73 ± 0.89	2.57 ± 2.54	3.23 ± 2.85	**/11.96
Ammonium [μM]	1.62 ± 1.51	1.44 ± 1.47	ns/0.36	1.62 ± 1.34	1.87 ± 1.90	1.20 ± 1.11	ns/1.07
DIN [μM]	2.78 ± 2.23	5.65 ± 3.43	**/13.51	2.35 ± 1.94	4.44 ± 3.34	4.43 ± 3.15	*/6.93
NO_3^-%	39.46 ± 22.10	67.05 ± 29.31	**/9.03	31.67 ± 16.47	53.69 ± 27.88	60.62 ± 29.5	**/9.26
N:P	12.58 ± 29.71	13.25 ± 12.92	ns/1.02	8.76 ± 5.82	18.89 ± 42.03	10.77 ± 11.1	ns/0.03
Phosphate [μM]	0.39 ± 0.23	0.61 ± 0.29	*/5.97	0.27 ± 0.07	0.57 ± 0.28	0.57 ± 0.30	***/20.17
Silicate [μM]	2.89 ± 1.71	9.51 ± 4.34	***/24.59	2.88 ± 1.85	4.18 ± 3.39	8.23 ± 4.95	**/13.53
DO [μM]	188.48 ± 19.7	126.26 ± 17.52	***/32.18	195.29 ± 13.95	172.81 ± 26.66	135.12 ± 31.23	***/24.14
DO%	89.16 ± 10.74	53.07 ± 7.80	***/33.46	94.19 ± 6.43	78.78 ± 14.89	58.44 ± 16.57	***/27.96
TRIX	5.59 ± 1.34	7.98 ± 0.44	***/29.98	4.93 ± 1.29	6.84 ± 1.23	7.40 ± 1.10	***/22.31

Variables: DIN (dissolved inorganic nitrogen), NO_3^-% (percentage of nitrate about DIN), DO (dissolved oxygen), DO% (oxygen saturation). p-Value significance levels: < 0.05 *; < 0.01 **; < 0.001 ***; ns: non-significant.

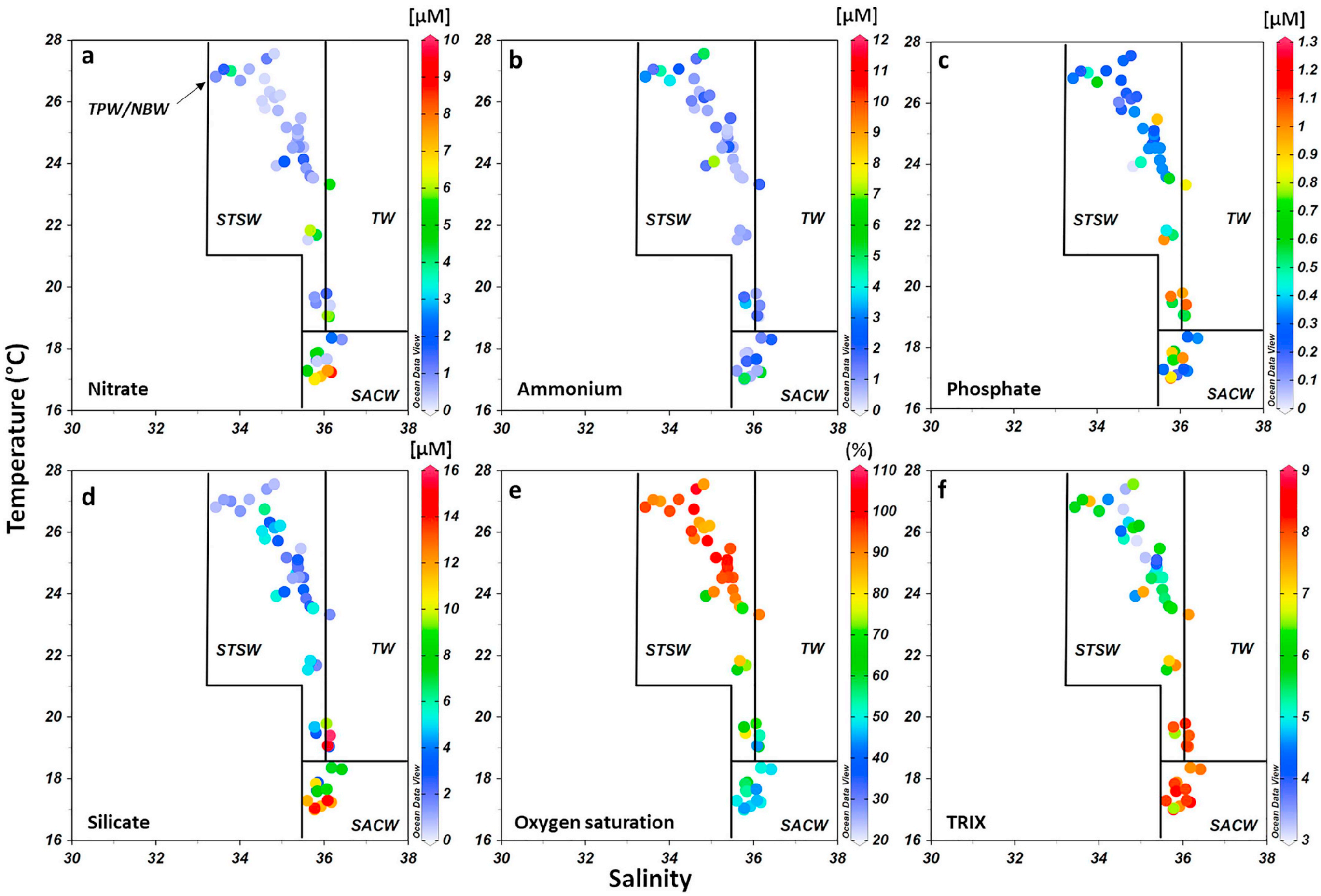

Fig. 4. TS diagram associated with the concentrations of (a) nitrate (μM), (b) ammonium (μM), (c) phosphate (μM), (c) silicate (μM), oxygen saturation (%) and TRIX in austral summer campaigns at the inner and mid continental shelf of Santa Catarina State, South Brazil Bight. STSW – Subtropical Shelf Water; TW – Tropical Water; SACW – South Atlantic Central Water; TPW – Tijucas River Plume Water; NBW – Florianópolis North Bay Channel Water.

Table 4

Regenerated nitrogen estimated in the SACW by the Libes (2009) and Braga and Muller (1998) methods for the summer on the inner and mid continental shelf of Santa Catarina State, South Brazil Bight. The observed nitrate was measured in situ and the expected values were calculated by the methods. The regenerated nitrogen is the difference between the observed and the expected nitrate. Nitrate and oxygen concentrations are in μM; oxygen saturation in %.

Year	Station	Observed nitrate	Expected nitrate Libes (2009)	Regenerated nitrogen Libes (2009)	Expected nitrate Braga and Muller (1998)	Regenerated nitrogen Braga and Muller (1998)	Oxygen concentration	Oxygen saturation
2014	50C	4.32	8.06	−3.74	5.55	−1.23	151.40	63.42
2014	50B	6.45	8.06	−1.61	5.86	0.59	148.27	62.12
2014	50A	1.50	5.72	−4.22	6.85	−5.35	138.00	57.53
2015	50C	6.57	13.00	−6.43	8.33	−1.76	122.81	50.56
2015	50B	7.05	2.34	4.71	9.11	−2.06	114.77	47.40
2015	50A	7.50	3.25	4.25	9.46	−1.96	111.20	46.14
2016	50C	6.62	11.05	−4.43	9.76	−3.14	108.07	44.54
2016	30C	0.35	12.87	−12.52	10.02	−9.67	105.40	44.03
2016	30B	0.88	4.42	−3.54	9.24	−8.36	113.43	48.07
2016	50B	5.04	4.03	1.01	8.72	−3.68	118.79	49.14
2016	30A	2.37	3.90	−1.53	8.72	−6.35	118.79	50.32
2016	50A	0.28	9.23	−8.95	7.68	−7.40	129.51	53.96

The mean and KW results are presented for each water mass and water column layer in Table 5. The values of each sample for the variables, namely, nitrate, ammonium, phosphate, silicate, DO% and TRIX in relation to water masses are shown in the TS diagrams (Fig. 7). Vertical profiles of DO are shown in the Fig. 10 (Appendix A) for each oceanographic campaign. The PPW was considered mostly as mesotrophic and the STSW as eutrophic by the mean TRIX of each water mass (Table 5).

Due to the PPW dominance all over the area in 2016, POM is presented just per layer of the water column. POC values ranged mainly between 200 and 600 $\mu g \cdot L^{-1}$ (Fig. 8a) and PON mainly between 50 and 100 $\mu g \cdot L^{-1}$ (Fig. 8b), with no significant differences between the layers (KW test: H = 2.67; and H = 1.72 respectively). Regarding the ratios, just POC:Chl-*a* showed differences along the water column (KW test: $p < 0.01$; H = 11.59). The values were < 100 at both surface (67.3 ± 10.73) and intermediate (85.05 ± 25.5) layers, but higher at the bottom (330.31 ± 192.64) (Fig. 8c). The C:N ratios ranged predominantly from 6 to 10 at the surface (6.2 ± 0.83), but between 3 and 6 at the intermediate (5.9 ± 1.17) and bottom (5.11 ± 0.61) layers (Fig. 8d).

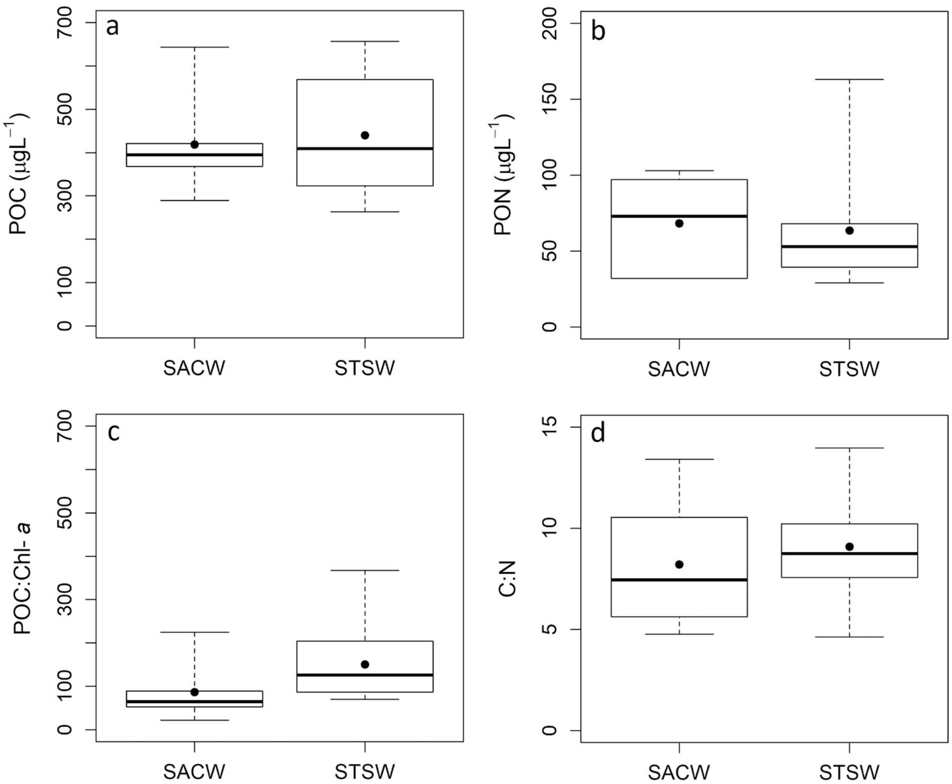

Fig. 5. Concentrations of (a) particulate organic carbon (POC), (b) particulate organic nitrogen (PON), (c) POC:Chl-*a* ratios and (d) elemental carbon to nitrogen ratios (C:N) during the summer campaign of 2016 at the inner and mid continental shelf of Santa Catarina State, South Brazil Bight at the SACW and STSW. Median (bold line) and mean (black dots) values are shown in the boxplot. Hinges are 25th and 75th percentiles. Whiskers are 5th and 95th percentiles.

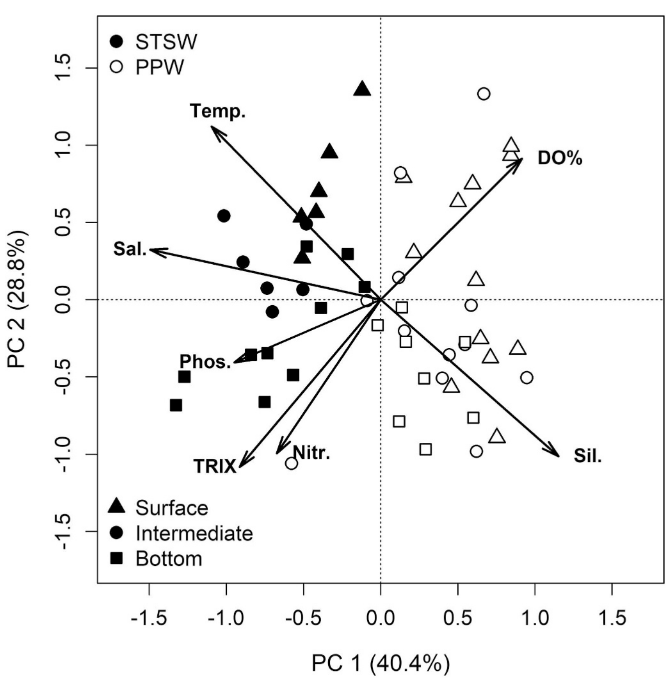

Fig. 6. Principal component analysis of the variables, namely, temperature (Temp.), salinity (Sal.), oxygen saturation (DOS), nitrate (Nitr.), Phosphate (Phos.), silicate (Sil.) and TRIX for the austral winter campaigns (2014, 2015 and 2016) on the inner and mid continental shelf of Santa Catarina State, South Brasil Bight. The water masses Subtropical Shelf Water (STSW – black) and South Atlantic Central Water (SACW – white) legend is on the upper left hand side; the water column layers (surface, intermediate and bottom) legend is on the bottom left hand side.

4. Discussion

There was a strong seasonal variability in the water mass distribution, leading to different nutrient availability, and therefore, carbon dynamics. During summer, the nitrate-rich SACW onshore bottom intrusions enriched the area, while nitrogen-loss by denitrification at the bottom layers controlled the primary production by nitrogen limitation. During winter, the silicate-rich PPW and regeneration process enhanced the primary production mostly at the upper layers because of the shallower euphotic zone. Silicate was a reliable proxy to monitor the PPW influence on the SC coast. The trophic index of SACW (eutrophic) revealed the highest potential for biological production, followed by the winter STSW (eutrophic), the mesotrophic PPW and the summer STSW.

Located in a transitional zone between the subtropical and temperate regions of the western boundary current system (Loder et al., 1998), the SC coast is a typical region of subtropical shelf waters marked by the seasonal variability in the water column stratification. Throughout the year, a strong stratification occurs during summer periods, decreasing to the weakest stratification patterns during the winter (Castro et al., 2006; Castro, 2014; Freire et al., 2017), thus, affecting the biogeochemical dynamics, such as the OM production and oxidation (Braga and Niencheski, 2006; Braga et al., 2008).

The hydrodynamics of the SBB resemble those found in the South Atlantic Bight (SAB), south-eastern USA, where surface salinity fronts and the Gulf Stream Water (GSM) bottom intrusions (as SACW in the SBB) affect the nutrient dynamics (Atkinson et al., 1984; Atkinson, 1985), plankton productivity (Yoder et al., 1983, 1985) and hence, phytoplankton biomass (Martins and Pelegri, 2006; Signorini and Mcclain, 2007). These similar influencing phenomena make the SAB an appropriate region to compare with our study area (Brandini et al., 2014).

Table 5
Mean (± standard deviation) values for all variables and results of Kruskal Wallis one-way analysis of variance (p: p-value/H: chi-squared) for the austral summer campaigns (2014, 2015 and 2016) on the inner and mid continental shelf of Santa Catarina State, South Brazil Bight. KW tested differences between factors water mass (PPW: Plata Plume Water; STSW: Subtropical Shelf Water) and amongst water column layer (surface, intermediate and bottom).

	STSW	PPW	KW (p/H)	Surface	Intermediate	Bottom	KW (p/H)
Temperature (°C)	18.96 ± 0.38	17.95 ± 0.59	***/23.95	18.48 ± 0.78	18.33 ± 0.8	18.25 ± 0.54	ns/2.12
Salinity	34.16 ± 0.35	32.93 ± 0.37	***/38.40	33.15 ± 0.71	33.47 ± 0.71	33.69 ± 0.64	ns/5.10
Nitrate [μM]	1.49 ± 0.81	1.05 ± 0.66	*/4.27	0.80 ± 0.49	1.21 ± 0.54	1.69 ± 0.92	***/14.60
Ammonium [μM]	1.52 ± 2.28	1.32 ± 1.02	ns/0.93	1.32 ± 1.20	1.23 ± 0.94	1.67.2.44	ns/0.20
DIN [μM]	3.02 ± 2.27	2.37 ± 1.12	ns/1.56	2.13 ± 1.26	2.44 ± 0.94	3.36 ± 2.38	*/7.49
NO_3^-%	57.70 ± 24.15	45.42 ± 18.31	*/3.85	42.83 ± 20.42	52.39 ± 19.64	56.06 ± 23.37	ns/4.49
N:P	7.75 ± 7.05	8.03 ± 5.83	ns/0.71	7.92 ± 7.53	7.33 ± 3.09	8.52 ± 7.52	ns/0.51
Phosphate [μM]	0.45 ± 0.20	0.32 ± 0.07	***/11.88	0.32 ± 0.09	0.34 ± 0.07	0.46 ± 0.23	**/10
Silicate [μM]	4.23 ± 2.01	8.49 ± 2.37	***/26.97	6.60 ± 3.46	6.51 ± 3.26	7.18 ± 2.53	ns/0.43
DO [μM]	193.48 ± 19.71	212.41 ± 35.8	**/10.10	224.5 ± 14.88	201.59 ± 42.22	188.02 ± 19.28	***/22.49
DO%	81.86 ± 8.42	87.57 ± 14.88	**/6.78	93.57 ± 5.83	83.93 ± 17.29	78.25 ± 7.55	***/24.58
TRIX	6.60 ± 0.61	5.94 ± 1.03	**/9.76	5.57 ± 0.98	6.38 ± 1.07	6.55 ± 0.46	*/8.47

Variables: DIN (dissolved inorganic nitrogen), NO_3^-% (percentage of nitrate about DIN), DO (dissolved oxygen), DO% (oxygen saturation). p-Value significance levels: < 0.05 *; < 0.01 **; < 0.001 ***; ns: non-significant.

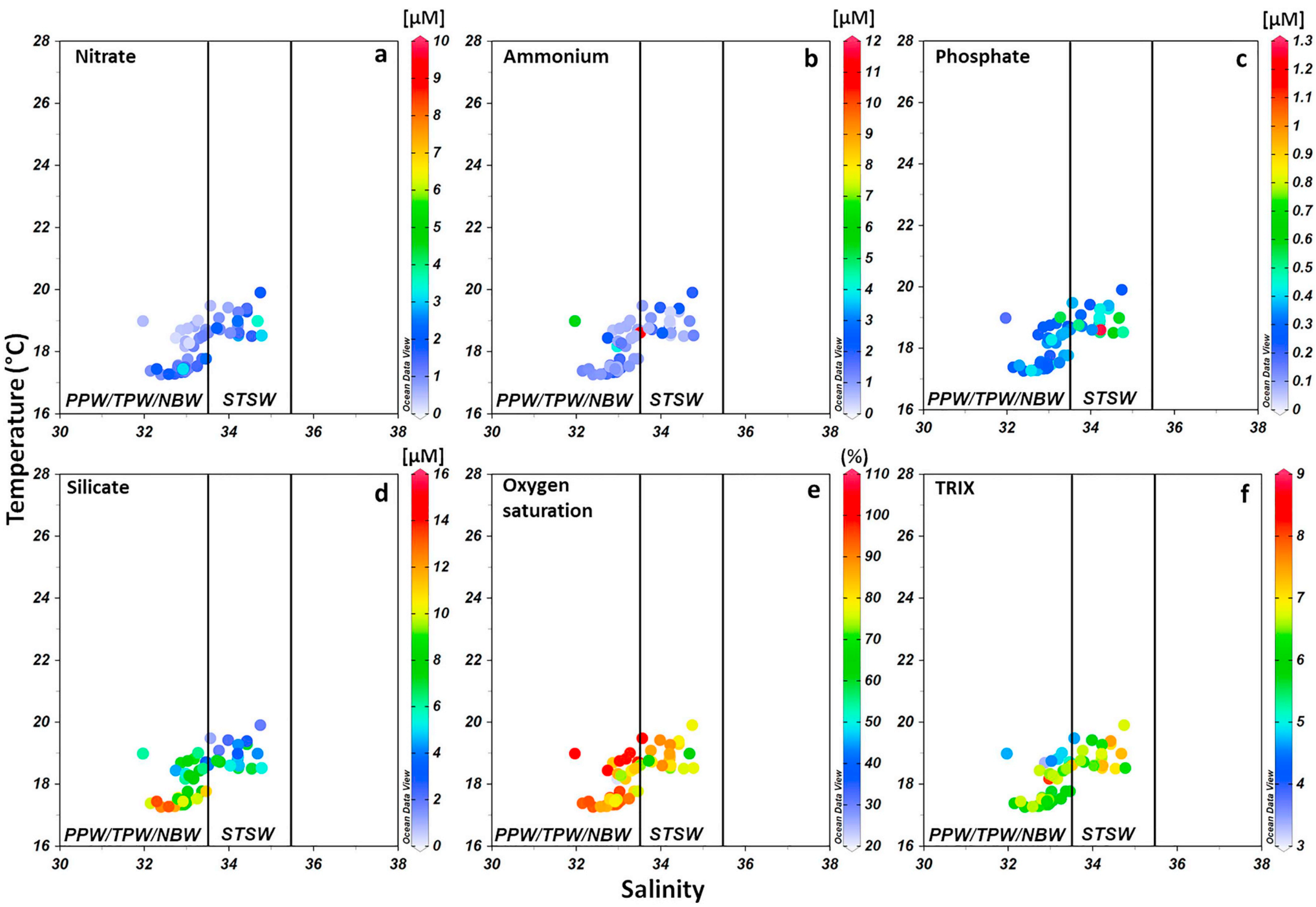

Fig. 7. TS diagram associated with the concentrations of (a) nitrate (μM), (b) ammonium (μM), (c) phosphate (μM), (c) silicate (μM), oxygen saturation (%) and TRIX in austral winter campaigns at the inner and mid continental shelf of Santa Catarina State, South Brazil Bight. STSW – Subtropical Shelf Water; PPW – Plata Plume Water; TPW – Tijucas Plume Water; and NBW – Florianópolis North Bay Channel Water.

4.1. Nutrient dynamics

Both summer and winter campaigns showed interannual variability of water masses. During summer, the SACW bottom intrusion moved closer to the coast (Freire et al., 2017), at least from 2015 to 2016. The 2014 campaign was carried out in the early fall, when SACW tends to be positioned farther away from the coast (Brandini et al., 2014). According to Brandini et al. (2014), on the SC coast, the SACW in early fall was positioned at the 70 m isobath, while our results showed it was in the bottom at the 50 m isobath. In 2015, SACW was at the intermediate and bottom layers of the 50 m isobath and at the bottom of the 30 m isobath—only in the second day of the campaign (stations 30A, 50A, 50B and 50C - campaign dates in Fig. 2)—possibly induced by upwelling-favourable northerly winds. Campos et al. (2013) using hydrographical data, satellite-derived wind stress and numerical simulations, showed that upwelling events in Cape Santa Marta—slightly southern

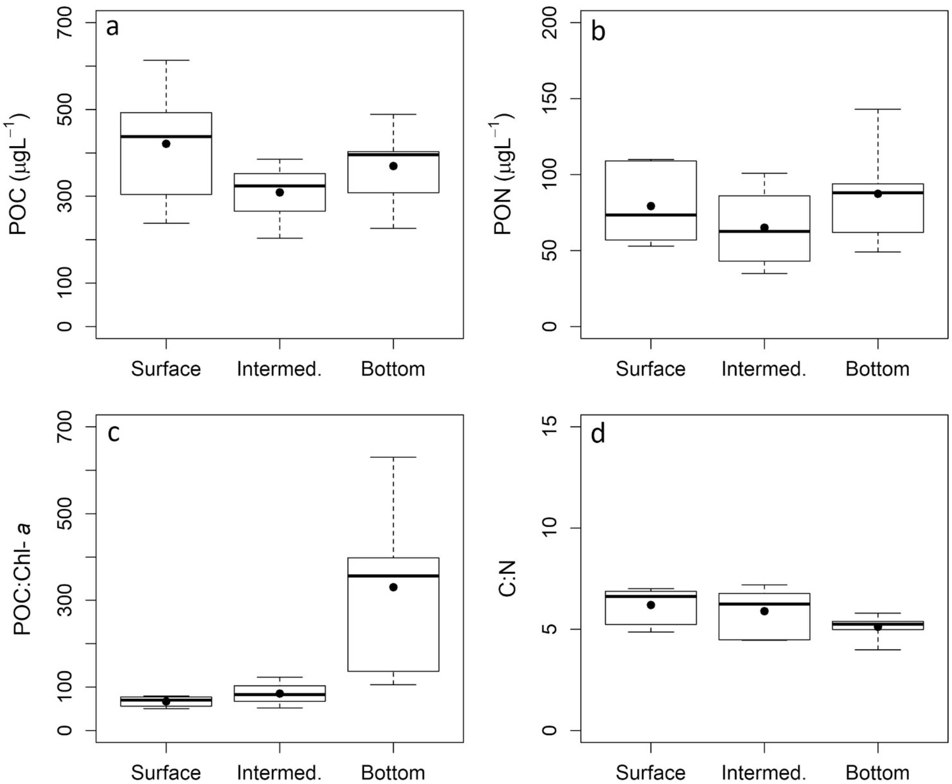

Fig. 8. Concentrations of (a) particulate organic carbon (POC), (b) particulate organic nitrogen (PON), (c) POC:Chl-*a* ratios and (d) elemental carbon to nitrogen ratios (C:N) during the winter campaign of 2016 at the three sampling depths (surface, intermediate and bottom). Median (bold line) and mean (black dots) values are shown in the boxplot. Hinges are 25th and 75th percentiles. Whiskers are 5th and 95th percentiles.

from our study area—started 20 to 30 h after the wind rotated to the northeast. In 2016, the northerly winds (between 2016-02-11 and 2016-02-15, see Fig. 2) favoured the SACW to reach up the vicinity of Tijucas Bay at the bottom layer (Freire et al., 2017). In 2015, but notably in 2016, the abundant rainfall on previous days favoured the TPW to reach the 30 m isobath (Freire et al., 2017).

The SACW deep intrusions were considered an important source of new nutrients to the SBB ecosystems (Braga and Niencheski, 2006; Braga et al., 2008; Brandini et al., 2018), mostly in the nitrate form (*sensu* Dugdale and Goering, 1967; Metzler et al., 1997). This phenomena is corroborated by the higher NO_3^-% in the deep SACW (Fontes et al., 2018) than in the STSW at the upper mixed layer (UML). Moreover, the phosphate and silicate concentrations followed the same pattern, higher in the SACW than in the STSW. The PCA negative correlation between nitrate, phosphate and silicate in relation to the temperature corroborates the nutrients supply by the colder SACW. On the other hand, in 2016, the high nitrate and ammonium concentrations (up to 3.95 and 4.49 respectively) at the 30 m isobath (at the surface) were probably associated to the TPW and NBW (Freire et al., 2017). Our nutrient concentrations are in accordance with those reported about the northern (Coelho-Souza et al., 2017) and southern SBB during SACW intrusions (Brandini, 1990; Braga et al., 2008; Fontes et al., 2018), like the GSW intrusions in the SAB (Atkinson et al., 1984; Atkinson, 1985).

During summer mineralization process might also have contributed to the autochthonous supply of regenerated nutrients. The SACW is characterized as an oxygen-rich water mass (Braga and Muller, 1998) and its onshore intrusion leads to an increase in the primary production at the base of the Zeu. The produced OM is then oxidized during the SACW displacement along the shelf, which is corroborated by oxygen depletion in the water column (Braga and Muller, 1998) and sediments (Valentin, 1992). Thus, when the SACW reaches the inner-shelf, it is even more nutrient-rich but oxygen depleted (Braga and Muller, 1998). Braga and Muller (1998) observed the regeneration during the SACW bottom intrusion in the SBB, Ubatuba region, and observed that the nutrient concentrations increased from the 300 m depth offshore to the inner-shelf. Nevertheless, despite this increase, they found a negative difference between the observed and the expected nitrate, calculated by the DO stoichiometry method, attributed probably to the denitrification process.

Our study also identified a nitrogen loss by the Libes (2009) and Braga and Muller (1998) methods in all summer campaigns, associated with low DO, DO%, and N:P ratios lower than the canonical Redfield ratio of 16:1 (Redfield et al., 1963) (see details in Table 3). Although not common, denitrification can occur under aerobic conditions (Robertson and Kuenen, 1984; Zhang et al., 2011). In an environment with low oxygen concentrations, if oxygen does not suppress the nitrate utilization, aerobic denitrification can occur simultaneously as a co-respiration of the two electron acceptors (Zumft, 1997) carried out by some facultative anaerobic organisms (Zehr and Ward, 2002). Indeed, phytoplankton aggregates can hold interior anoxia core where anaerobic denitrification and nitrate reduction can occur, which can be intensified in water layers with low oxygen content and high nitrate (Klawonn et al., 2015) and POM concentrations (Babbin et al., 2014). In coastal zones some processes can favour denitrification, e.g. deep intrusion of a cold, nutrient-rich water mass, which promotes a thermal stratification limiting the bottom oxygenation with an increase in OM availability by primary production under favourable nutritional conditions. The POC and the Chl-*a* data reported by Freire et al. (2017) at these campaigns are relatively high compared to other studies in the SBB (Brandini, 1990; Brandini et al., 2014), in both UML and bottom layers. Therefore, the considerable availability of nitrate and POM combined with low DO on the SACW created ideal conditions for denitrification in the bottom waters of the central inner- and mid-shelf of SC.

The range of the nitrate loss is in accordance with those found by Braga and Muller (1998). Positive differences in the observed and expected nitrate estimated by the Libes (2009) method were caused by the very low phosphate concentrations, which was probably removed from the water column by adsorption and/or flocculation by thin sediments. Finally, OM regeneration via denitrification at bottom layers is a source of nutrients, which supports the maintenance of the Chl-*a* maximums in depth (Ediger et al., 2005). Nevertheless, it is important to point out that the methods utilized here are relied on some basic assumptions, hence, more studies are necessary to accurately investigate this process.

In winter, the increase of PPW over the region between 2014 and 2016 (Freire et al., 2017) was probably associated with the wind field variability, which was considered as the main factor controlling the PPW behaviour (Piola et al., 2005; Möller et al., 2008). The PPW is considered an important source of nutrients along their northward reach, mostly with phosphate and silicate, which are considered PPW tracers by its PCA negative correlations with salinity (Braga et al., 2008). In our study, however, only silicate presented a negative correlation with salinity, while phosphate showed its highest concentrations at the saltier STSW—suggesting other phosphate sources to the SC coast during the austral winter. The PPW nutrients are generally consumed by phytoplankton assimilation along the way from Uruguayan to Brazilian coastal waters, and thus, a small fraction reaches the SC coast (Brandini, 1990; Braga et al., 2008). Moreover, the flocculation and adsorption process contributes to the colloidal and particulate phosphorus phases, mitigating the signal from the dissolved phosphate (Braga et al., 2008). On the contrary, the silicate seems to be more conservative. Its concentrations raised following the PPW approximation to the area from 2014 to 2016 (KW test: $p < 0.001$ between years). Therefore, silicate may represent itself as a more appropriate proxy to monitor the PPW influence on the SC coast. Our observed silicate concentrations are in accordance with those reported by Braga et al. (2008) and Fontes et al. (2018) on the SC coast in the same season.

While silicate was higher at the PPW, nitrate (Fontes et al., 2018) and phosphate were higher at the STSW. Nevertheless, we must also consider the vertical distribution, since different biogeochemical processes were observed associated with an interannual variability on water masses along the water column. While silicate and ammonium did not show significant differences along the water column, nitrate and phosphate increased towards the bottom, followed by a sharp decrease of DO%, which reached the minimum down to 20% in the deepest layer. Braga et al. (2008) associated DO% values below 93% with regeneration processes, i.e. above the observed value for the intermediate (83 ± 17.29%) and bottom layers (78.25 ± 7.55%). These results therefore suggest that OM regeneration is a key process in the bottom layers. The high NO_3^-% at bottom layers, notably in 2014 (71.16 ± 11.91%), suggests that the regenerated ammonium is readily oxidized to nitrite and nitrate forms, also contributing to the decreasing DO% levels. At the surface, our DO% values were in accordance with those reported by Braga et al. (2008) and Ito et al. (2016) in their winter campaigns on the SC coast.

4.2. Primary production and carbon dynamics

The primary production in the SBB is mostly regenerated (*sensu* Dugdale and Goering, 1967) over the year (Metzler et al., 1997), as in the SAB (Atkinson et al., 1984; Atkinson, 1985). During winter, the PPW nutrients enhance the primary production, mostly in the upper layers because of the shallower Zeu (Ciotti et al., 1995; Brandini et al., 2007). We observed the phytoplankton-dominated POM at the surface and intermediate layers in the 2016 winter campaign by both POC:Chl-*a* and C:N ratios, which is in accordance with the Chl-*a* maximums in the upper layers by other authors in the SBB under PPW influence (Brandini, 1990; Brandini et al., 2014).

The POM characteristics also suggest the occurrence of a vertical trophic profile in winter. Overall, those phytoplankton biomass greater than $> 5\,\mu g{\cdot}L^{-1}$ observed by Freire et al. (2017) in the same sampling water campaign were concomitant to higher DO% in upper layers. On the other hand, the rising nutrients and decreasing DO% were observed towards the bottom, where the POM was predominantly heterotrophic accordingly with the C:N ratios in intermediate and bottom layers (Liénart et al., 2016). At these depths, the POM is remineralized by bacteria, returning nutrients to water column and to the upper layers by tidal and wind mixing (Freire et al., 2017). Therefore, besides the PPW nutrient contribution, the importance of the regeneration process for the nutrients supply can be clearly recognised, which supports a regenerative primary productivity during the winter periods. The high PCA negative correlation of TRIX in relation to the DO% reinforce this feature, indicating that TRIX was determined mainly by this variable, associated with the OM oxidation in the bottom layers. Overall, the TRIX showed higher potential for biological production in the STSW than in PPW, though STSW is restricted to a depth higher than the Zeu, covered by PPW.

On the other hand, the regenerated primary production is temporarily alternated with the new production during the summer SACW onshore bottom intrusions (Metzler et al., 1997), like the GSW intrusions in the SAB (Atkinson et al., 1984; Atkinson, 1985). During these intrusions at the bottom layers, the deepest Zeu meets the nutricline, providing ideal conditions to the primary producers mostly at the base of the thermocline/nutricline (Brandini, 1990; Brandini et al., 2014) as observed here. Moreover, the sinking phytoplankton cells along the water column accumulated at this layer, creating a Deep Chl-*a* Maximum (DCM, *sensu* Brandini et al., 2014; Ediger et al., 2005), and further by the increase of the Chl-*a*:cell content to become adapted to low light conditions (Richardson et al., 1983; Reynolds, 2006). The DCM is not well defined at the near-shore like at the mid and the outer shelf regions. It is noteworthy that the phytoplankton dominated the POM all over the water column (POC:Chl-*a* < 200; C:N 6–10). However, the POC:Chl-*a* in the SACW characterizes the POM as living phytoplankton (< 100), while in the STSW the ratio does not discriminate them as living, but identifies just as the phytoplankton-dominated POM (Liénart et al., 2016). Therefore, this phenomenon suggests a higher phytoplankton contribution to the total POM in the SACW, which establishes the DCM in the layers occupied by this water masses. This is corroborated by Freire et al. (2017), who found, in the same sampling water campaign, the highest Chl-*a* content at the intermediate and bottom layers of the inner, but mostly mid-shelf at the 50 m isobath associated with SACW. Our findings are in accordance with the other studies in the SBB (Odebrecht and Djurfeldt, 1996; Queiroz et al., 2004; Brandini et al., 2014) as well as in the SAB (Yoder et al., 1985).

The trophic index of SACW revealed high potential for biological productivity (eutrophic, but very close to 8.01 – hyper-eutrophic) because of the new and regenerated nutrients, which supported the maintenance of the DCM. TRIX correlated with the corresponding state variables (PCA) (Vollenweider et al., 1998) also revealed that it was mainly determined by the DO%, associated with the oxygen consumption by OM oxidation. At the UML, the mean TRIX for the STSW (< 6.01) showed lower potential for biological production. However, under large rainfall conditions, the drainage from TPW and NBW—surrounded by urbanized and industrialized areas with precarious sewage treatment—can increase the ammonium concentrations over the region (Freire et al., 2017), and hence, TRIX, as observed in the 30 m isobath in 2016 (up to 7.3 TRIX units).

However, despite the high potential for biological production estimated by the TRIX trophic status, the SACW and winter STSW were located in the lower limit or below the Zeu, which reduced its potential due to low light availability. While the upper layers were light favourable and nutrient limited, the bottom layers turned to be nutrient abundant but light-limiting (Dugdale, 1967), as observed by Brandini (1990) at the SBB and Verity et al. (1993) at the SAB.

Nevertheless, the potential for biological production by the TRIX can be associated with the mean rates of primary production at the SBB, which range between $< 0.04\,gC{\cdot}m^{-2}{\cdot}d^{-1}$ in an ammonium-based regenerated production and $> 0.5\,gC{\cdot}m^{-2}{\cdot}d^{-1}$ in a nitrate-based new production (Brandini, 1990; Gaeta and Brandini, 2006) at fronts, created by SACW and PPW intrusions (Brandini et al., 2018 and references therein). Following the Nixon (1995) and Cloern et al. (2014) classifications, the winter STSW (eutrophic) has potential to produce 0.81–1.36 $gC{\cdot}m^{-2}{\cdot}d^{-1}$, while PPW (mesotrophic) 0.27–0.81 $gC{\cdot}m^{-2}{\cdot}d^{-1}$. During summer, the STSW has potential to produce just up to

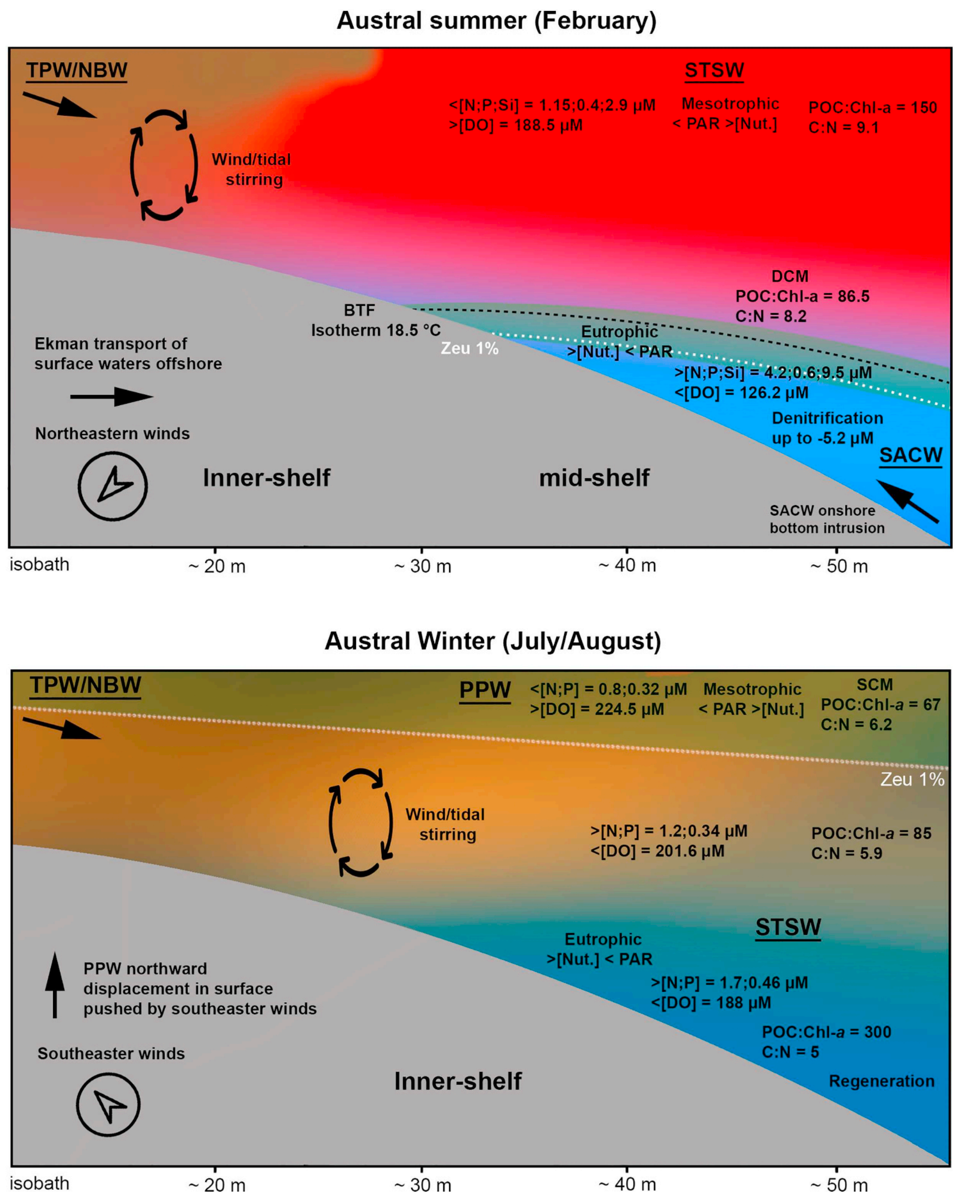

Fig. 9. Conceptual model of the hydrographic and biogeochemical dynamics during the austral summer and winter on the inner and mid continental shelf of Santa Catarina State, South Brazil Bight, between the 30 and 50 m isobaths. In summer, the limit between the inner- and mid-shelf was determined by the bottom thermal front (BTF – isotherm of 18.5 °C, black dashed line), positioned approximately at the 30 m isobath, while in winter, since the BTF is positioned farther from the coast, the area represent the inner-shelf. Mean values of nitrate, phosphate, silicate, dissolved oxygen, POC:Chl-*a* and C:N ratios are presented by the water mass—in summer: STSW (red) and SACW (blue); in winter: PPW (brown) and STSW (blue). TPW and NBW runoff are just illustrative (no data). The maximums of Chl-*a* is indicated by green color: in summer, the DCM is positioned between the BTF (thermocline) and the Zeu depth, while in winter, the surface Chl-*a* maximum (SCM) layer is between the surface and the Zeu. The Zeu is represented by a white dotted line, which represents 1% of photosynthetically active radiation (PAR). The potential for biological production by the trophic status infer about its effectiveness by the relation of the availability of nutrients and PAR. The elaboration of the conceptual models was based on supplementary information from Brandini et al. (2014) and Freire et al. (2017). (For interpretation of the references to color in this figure legend, the reader is referred to the web version of this article.)

0.81 $gC{\cdot}m^{-2}{\cdot}d^{-1}$ (mesotrophic), while SACW between 0.81 to > 1.36 $gC{\cdot}m^{-2}{\cdot}d^{-1}$, since some TRIX data were > 8.01 (hyper-eutrophic). Therefore, we assume that SACW has the highest potential for biological production of all the other water masses. During the SACW onshore intrusions, the large phytoplankton cells at the DCM (Guenther et al., 2008) works as a food source for most filter feeders, and is predicted a simple and short trophic system with low energetic losses (Odebrecht and Djurfeldt, 1996). Therefore, an energy parcel of new production is transferred to higher trophic levels more efficiently (Mann and Lazier, 2006) during this period, contributing to the fishery productivity. In contrast, a more complex food web may be found in the UML associated with low Chl-*a* and small phytoplankton cells (Odebrecht and Djurfeldt, 1996; Guenther et al., 2008).

5. Conclusions

Wind-driven processes, such as the SACW onshore bottom intrusions during the summer and the PPW northward displacement during the winter are important processes that fertilise the inner- and mid-shelf of SC enhancing the primary production. However, the supply of autochthonous nutrients by regeneration processes is the most important to support primary production along the year. Nutrients enrichment towards the bottom associated with low DO and DO% values revealed the potential of regeneration in deep layers in both seasons. During the austral winter, the PPW proved to be an important source of silicate to the region, while nitrate and phosphate seemed to be mainly supplied by the regeneration in the bottom layers and then moved to the surface by wind and tidal mixing. During the austral summer, the system temporarily transitions to new production provided by the nutrient input of the SACW intrusions, forming a DCM (POC:Chl-*a* < 100) at the base of thermocline. The SACW reaches the mid- and inner-shelf nutrient-rich, but with relatively low levels of oxygen because of a regeneration process in the bottom. However, denitrification also occurs leading to a system nitrogen loss, controlling the primary production by nitrogen limitation. The TRIX trophic status indicated high potential for biological production, mostly at the SACW and winter STSW, however, the potential is not totally utilized because of the light limitation. Finally, the greater coverage of SACW and PPW over the area seemed to intensify processes like primary production, hence, regeneration of the produced OM. However, it is noteworthy that a longer time series is necessary to accurately evaluate the interannual variability and consequences of climatic oscillations on water mass dynamics and ecosystem responses. The results of this work were summarized in two conceptual models to represent the hydrographic and biogeochemical processes and dynamics during the austral summer and winter (Fig. 9). The elaboration of the conceptual models were based on supplementary information from Brandini et al. (2014) and Freire et al. (2017).

Acknowledgements

Our special thanks go to the coordinating committee and all the scientists involved in the MAArE project for providing the majority of the data used in this work. The realization of the MAArE project is a condition indicated by ICMBio within the ambit of IBAMA's environmental licensing process. We extend our thanks to Gabriel S. de M. Silva who kindly made the wind stick plots (Fig. 2), and Danae Erdosi who made the study area map (Fig. 1). Luís H. Bordin was supported by the Coordination of Improvement of Higher Level Personnel (CAPES project process n° 1636498) and National Institute of Science and Technology - Integrated Oceanography and Multiple Uses of the Continental Shelf and Adjacent Ocean - Center for Integrated Oceanography (INCT-Mar COI project n° 400551/2014-4). Andrea S. Freire received research grants from the National Council for Scientific and Technological Development (CNPq projects 312644/2013-2 and 311994/2016-4).

Appendix A

Vertical profiles of temperature, salinity, dissolved oxygen and Zeu depth (Fig. 10). The complete database is available on the MAArE project (MAArE, 2017) website.

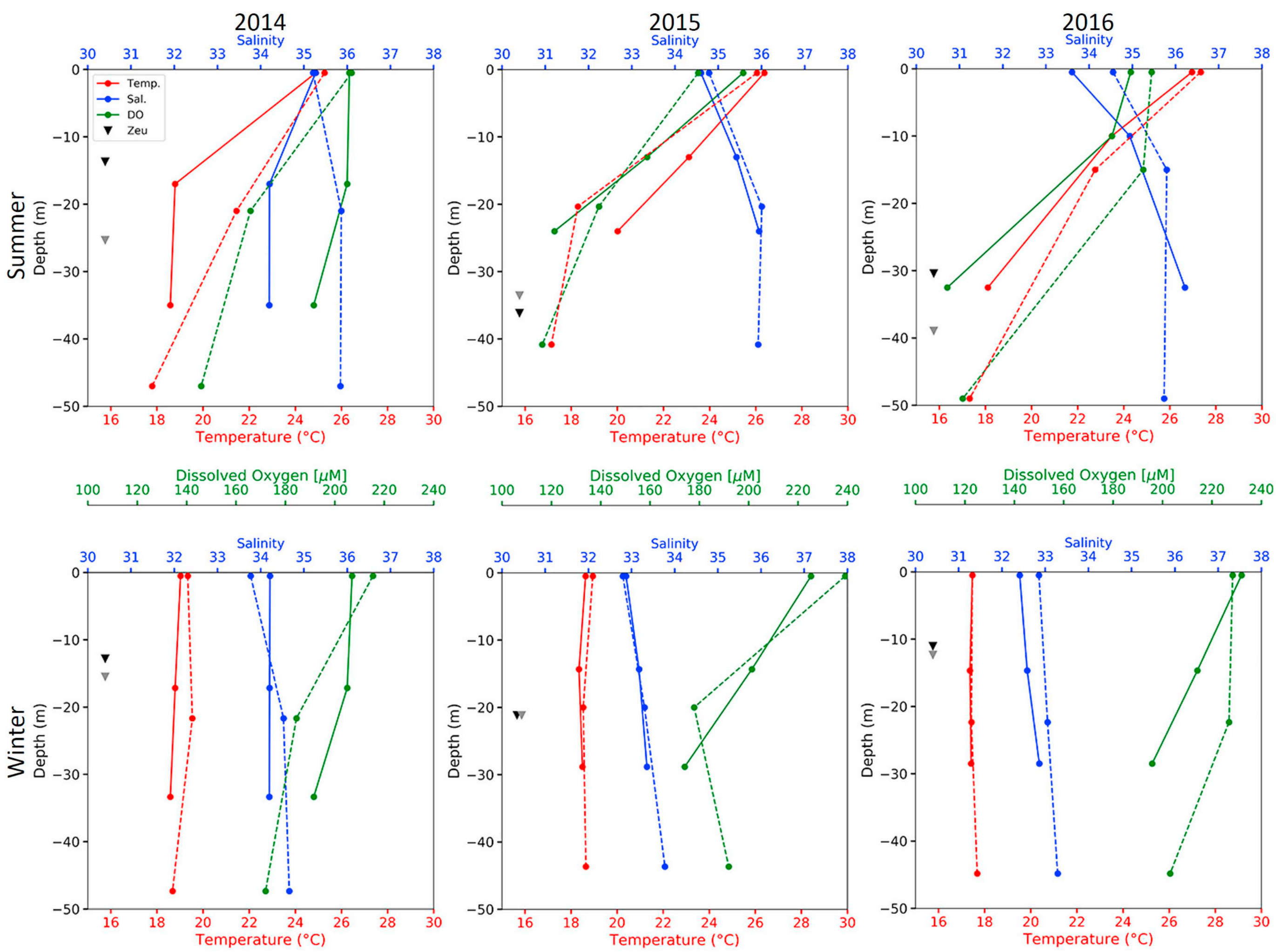

Fig. 10. Vertical profiles of temperature (Temp. – red), salinity (Sal. – blue), dissolved oxygen (DO – green) and euphotic zone depth (Zeu – triangle) of each sampling campaign (2014, 2015 and 2016 – columns) during the austral summer and winter (seasons – rows) on the inner and mid continental shelf of Santa Catarina State, South Brazil Bight. Mean values per water column layer (surface, intermediate and bottom) and sampling stations disposed at the 30 m isobath (continuous line and black triangle) and 50 m isobath (dashed line and gray triangle). (For interpretation of the references to color in this figure legend, the reader is referred to the web version of this article.)

References

Alvarez-Salgado, X.A., 1993. Mecanismos de transporte e balance biogeoquímico do nitrogeno na Ría de Arousa, Tese de doutorado. Universidade de Santiago de Compostela, Espanha (196pp. + anexo).

Atkinson, L.P., 1985. Hydrography and nutrients of the southeastern U.S. continental shelf. In: Atkinson, L.P., Menzel, D.W., Bush, K.A. (Eds.), Oceanography of the Southeastern Continental U.S. Shelf, Coastal Estuarine Sciences. vol. 2. AGU, Washington D. C., pp. 77–92. https://doi.org/10.1029/CO002p0077.

Atkinson, L.P., O'Malley, P.G., Yoder, J.A., Paffenhöfer, G.-A., 1984. The effect of summertime shelf break upwelling on nutrient flux in southeastern United States continental shelf waters. J. Mar. Res. 42, 969–993. https://doi.org/10.1357/002224084788520756.

Babbin, A.R., et al., 2014. Organic matter stoichiometry, flux, and oxygen control nitrogen loss in the ocean. Science 344, 406–408.

Bergo, N.M., Signori, C.N., Amado, A.M., Brandini, F.P., Pellizzari, V.H., 2017. The partitioning of carbon biomass among the pico- and nano-plankton community in the south Brazilian Bight during a strong summer intrusion of South Atlantic Central Water. Front. Mar. Sci. 4, 1–12. https://doi.org/10.3389/fmars.2017.00238.

Braga, E.S., Muller, T., 1998. Observation of regeneration of nitrate, phosphate and silicate during upwelling off Ubatuba, Brazil. Cont. Shelf Res. 18 (8), 915–922. https://doi.org/10.1016/S0278-4343(98)00002-8.

Braga, E.S., Niencheski, L.F.H., 2006. Composição das massas de água e seus potenciais produtivos na área entre o Cabo de São Tomé (RJ) e o Chuí (RS). In: Rossi-Wongtschowiski, C.L.D., Madureira, L.S.P. (Eds.), O ambiente Oceanográfico da Plataforma Continental e do talude na Região Sudeste-Sul do Brasil. Edusp, São Paulo, pp. 161–218.

Braga, E.S., Chiozzini, V.G., Berbel, G.B.B., Maluf, J.C.C., Aguiar, V.M.C., Charo, M., Molina, D., Romero, R., Eichler, B.B., 2008. Nutrients distribution over the southeastern South Atlantic continental shelf from Mar del Plata (Argentina) to Itajaí (Brazil): winter–summer aspects. Cont. Shelf Res. 28, 1649–1661.

Brandini, F.P., 1990. Hydrography and characteristics of the phytoplankton in shelf and oceanic waters off southeastern Brazil during winter (July/August 1982) and summer (February/March 1984). Hydrobiologia 196, 111–148(https://link.springer.com/content/pdf/10.1007/BF00006105.pdf).

Brandini, F.P., Silva, A.S., Silva, E.T., Kolm, H., 2007. Sources of nutrients and seasonal dynamics of chlorophyll in the inner shelf off Paraná State – South Brazil Bight. J. Coast. Res. 23 (5), 1131–1140. https://doi.org/10.2112/04-0360.1.

Brandini, F.P., Jr, M.N., Simião, M., Codina, J.C.U., Noernberg, M.A., 2014. Deep chlorophyll maximum and plankton community response to oceanic bottom intrusions on the continental shelf in the South Brazilian Bight. Cont. Shelf Res. 89, 61–75. https://doi.org/10.1016/j.csr.2013.08.002.

Brandini, F.P., Tura, P.M., Santos, P.P.G.M., 2018. Ecosystem responses to biogeochemical fronts in the South Brazil Bight. Prog. Oceanogr. 164, 52–62. https://doi.org/10.1016/j.pocean.2018.04.012.

Campos, E., Velhote, D., Silveira, I.C.A., 2000. Shelf break upwelling driven by Brazil current cyclonic meanders. Geophys. Res. Lett. 27 (6), 751–754. https://doi.org/10.1029/1999GL010502.

Campos, P.C., Moller, O.O., Piola, A.R., Palma, E.D., 2013. Seasonal variability and coastal upwelling near Cape Santa Marta (Brazil). J. Geophys. Res. Oceans 118, 1420–1430. https://doi.org/10.1002/jgrc.20131.

Castro, B.M., 2014. Summer/winter stratification variability in the central part of the South Brazil Bight. Cont. Shelf Res. 89, 15–23. https://doi.org/10.1016/j.csr.2013.12.002.

Castro, B.M., Miranda, L.B., 1998. Physical oceanography of the western atlantic continental shelf located between 41N and 341S – coastal segment (4,W). In: Robinson, A., Brink, K. (Eds.), The Sea. The Global Coastal Ocean: Regional, vol. 11.

Castro, B.M., Lorenzzetti, J.A., Silveira, I.C.A., Miranda, L.B., 2006. Estrutura termo-halina e circulação na região entre o Cabo de São Tomé (RJ) e o Chuí (RS). In: Rossi-Wongtschowski, C.L.B., Madureira, L.S.-P. (Eds.), O ambiente oceanográfico da plataforma continental e do talude na região Sudeste-Sul do Brasil. Editora da Universidade de São Paulo, São Paulo, pp. 11–120. https://www.scopus.com/record/display.uri?eid=2-s2.0-66549127534&origin=inward&txGid=2db53d9b3183c105ad3688644fd131f1.

Ciotti, A.M., Odebrecht, C., Fillmann, G., Möller Jr., O.O., 1995. Freshwater outflow and subtropical convergence influence on phytoplankton biomass on the Southern Brazilian continental shelf. Cont. Shelf Res. 15 (14), 1737–1756. https://doi.org/10.1016/0278-4343(94)00091-Z.

Cloern, J.E., Foster, S.Q., Kleckner, A.E., 2014. Phytoplankton primary production in the world's estuarine-coastal ecosystems. Biogeosciences 11, 2477–2501. https://doi.org/10.5194/bg-11-2477-2014.

Coelho-Souza, S.A., et al., 2017. Seasonal sources of carbon to the Brazilian upwelling system. Estuar. Coast. Shelf Sci. 194, 162–171. https://doi.org/10.1016/j.ecss.2017.06.013.

Cole, G.A., Weihe, P.E., 2015. Textbook of Limnology. 2015 Waveland Press.

Dodge, Y., 2008. Kruskal-Wallis test. In: The Concise Encyclopedia of Statistics. Springer, New York, NY. https://doi.org/10.1007/978-0-387-32833-1.

Dugdale, R.C., 1967. Nutrient limitation in the sea: dynamics, identification and significance. Limnol. Oceanogr. 12, 685–695. https://doi.org/10.4319/lo.1967.12.4.0685.

Dugdale, R.C., Goering, J.J., 1967. Uptake of new and regenerated forms of nitrogen in primary productivity. Limnol. Oceanogr. 12, 196–206.

Ediger, D., Tugrul, S., Yilmaz, A., 2005. Vertical profiles of particulate organic matter and its relationship with chlorophyll-a in the upper layer of the NE Mediterranean Sea. J. Mar. Syst. 55, 311–326. https://doi.org/10.1016/j.jmarsys.2004.09.003.

Falkowski, P.G., Raven, J.A., 2007. Aquatic Photosynthesis. Princeton University Press, Princeton.

Fontes, Maria Luiza S., Berri, Alexandre, Carvalho, Melissa, Fonseca, Alessandra L.O., Antônio, Regina V., Freire, Andrea S., 2018. Bacterioplankton abundance and biomass stimulated by water masses intrusions over the Southern Brazilian Shelf (between 25°57′S and 29°24′S). Cont. Shelf Res. https://doi.org/10.1016/j.csr.2018.05.003.

Freire, S.F., Varela, A.R.D., Fonseca, L.D., Menezes, B.S., Fest, C.B., Obata, C.S., Gorri, C., Franco, D., Machado, E.C., De Barros, G., Molessani, L.S., Santos Madureira, L.A., Coelho, M.P., Carvalho, M., Pereira, T.L., 2017. O Ambiente Oceanográfico. In: Segal, B., Freire, A.S., Lindner, A., Krajevski, J.P., Soldateli, M. (Eds.), Monitoramento da Reserva Biológica Marinha do Arvoredo e Entorno (MAArE). Universidade Federal de Santa Catarina, Florianópolis, pp. 159–200.

Gaeta, S.A., Brandini, F.P., 2006. Produção primária do fitoplâncton na região entre Cabo de São Tomé (RJ) e o Chuí (RS). In: Rossi-Wongtschowski, C.L.B., Madureira, L.S.-P. (Eds.), O ambiente oceanográfico da plataforma continental e do talude na região Sudeste-Sul do Brasil. Editora da Universidade de São Paulo, São Paulo, pp. 219–264.

Gérikas-Ribeiro, C., Santos, A.L., Marie, D., Pelizzati, V.H., Brandini, F.P., Vaulot, D., 2016. Pico and nanoplankton abundance and carbon stocks along the Brazilian Bight. PeerJ 4. https://doi.org/10.7717/peerj.2587.

Giering, L.C.S., Sanders, R., Lampitt, R.S., Anderson, T.R., Tamburini, C., Boutrif, M., Zubkov, M.V., Marsay, C.M., Henson, S.A., Saw, K., Cook, K., Mayor, D.J., 2014. Reconciliation of the carbon budget in the ocean's twilight zone. Nature 507 (7493), 480–483. https://doi.org/10.1038/nature13123.

Gordon, D.C., Boudreau, P.R., Mann, K.H., Ong, J.-E., Silvert, W., Smith, S.V., Wattayakorn, G., Wulff, T., Yanagi, T., 1996. LOICZ Biogeochemical Modelling Guidelines. Den Burg (The Netherlands): LOICZ Reports and Studies no. 5.LOICZ Biogeochemical Modelling Guidelines. Den Burg (The Netherlands): LOICZ Reports and Studies no. 5.

Grasshoff, K., Kremling, K., Ehrhardt, M., 1983. Methods of Seawater Analysis, 3rd ed. Verlag Chemie, Weinheim.

Guenther, M., Gonzalez-Rodriguez, E., Carvalho, W.F., Rezende, C.E., Mugrabe, G., Valentin, J.L., 2008. Plankton trophic structure and particulate organic carbono production during a coastal downwelling-upwelling cycle. Mar. Ecol. Prog. Ser. 363, 109–119.

Honjo, S., Manganini, S.J., Krishfield, R.A., Francois, R., 2008. Particulate organic carbon fluxes to the ocean interior and factors controlling the biological pump: a synthesis of global sediment trap programs since 1983. Prog. Oceanogr. 76 (3), 217–285. https://doi.org/10.1016/j.pocean.2007.11.003.

INMET - Instituto Nacional de Meteorologia, 2017. [online] Inmet.gov.br. Available at http://www.inmet.gov.br/portal/index.php?r=bdmep/bdmep , Accessed date: November 2018.

Ito, R.G., Garcia, C.A.E., Tavano, V.M., 2016. Net sea-air CO_2 fluxes andmodelled pCO_2 in the southwestern subtropical Atlantic continental shelf during spring 2010 and summer 2011. Cont. Shelf Res. 119, 68–84. https://doi.org/10.1016/j.csr.2016.03.013.

Klawonn, I., et al., 2015. Aerobic and anaerobic nitrogen transformation processes in N2-fixing cyanobacterial aggregates. ISME J. 9, 1456–1466. https://doi.org/10.1038/ismej.2014.232.

Libes, S., 2009. Organic biogeochemistry: the marine nitrogen and phosphorus cycles. In: Introduction to Marine Biogeochemistry, Second edition. Elsevier, Academic Press, San Diego California, pp. 661–708. https://www.elsevier.com/books/introduction-to-marine-biogeochemistry/libes/978-0-12-088530-5.

Liénart, N., Susperregui, P., Rouaud, V., Cavalheiro, J., David, V., Del Amo, Y., Duran, R., Lauga, B., Monperrus, M., Pigot, T., Bichon, S., Charlier, K., Savoye, N., 2016. Dynamics of particulate organic matter in a coastal system characterized by the occurance of marine mucilage – a stable isotope study. J. Sea Res. 116, 12–22. https://doi.org/10.1016/j.seares.2016.08.001.

Loder, J.W., Boicourt, W.C., Simpson, J.H., 1998. Western ocean boundary shelves coastal segment (W). In: Robinson, A.R., Brink, K.H. (Eds.), The Sea. vol. 11. John Wiley & Sons, Inc., New York, NY, pp. 3–27. https://www.scopus.com/record/display.uri?eid=2-s2.0-84975491150&origin=inward&txGid=8debf7ce764d24c25d3d02f385bcc5f7.

MAArE, 2017. Monitoramento Ambiental da Reserva Biológica Marinha do Arvoredo e Entorno. WWW page. http://www.maare.ufsc.br/en/.

Mann, K.H., Lazier, J.R.N., 2006. Dynamics of Marine Ecosystems: Biological-physical Interactions in the Oceans, 3rd ed. Blackwell Publishing, Malden, Ma & Oxford, UK. https://onlinelibrary.wiley.com/doi/book/10.1002/9781118687901.

Martins, A.M., Pelegri, J.L., 2006. CZCS chlorophyll patterns in the South Atlantic Bight during low vertical stratification conditions. Cont. Shelf Res. 26, 429–457. https://doi.org/10.1016/j.csr.2005.11.012.

Matsuura, Y., 1986. Contribuição ao estudo da estrutura oceanográfica da região sudeste entre cabo frio (RJ) e cabo de santa marta grande (SC). Ciência e Cultura 38 (8), 1439–1450.

Metzler, P.M., Glibert, P.M., Gaeta, S.A., Ludlam, J.M., 1997. New and regenerated production in the South Atlantic off Brazil. Deep-Sea Res. I 44, 363–384. https://doi.org/10.1016/S0967-0637(96)00129-X.

Miranda, L.B., 1982. Análise de massas de água da plataforma continental e da região oceânica adjacente: Cabo de São Tomé (RJ) e Ilha de São Sebastião (SP). Tese de Livre-Docência. Universidade de São Paulo, Instituto Oceanográfico (123p).

Möller, O.O., Piola, A.R., Freitas, A.C., Campos, E.J.D., 2008. The effects of river discharge and seasonal winds on the shelf off southeastern South America. Cont. Shelf Res. 28, 1607–1624. https://doi.org/10.1016/j.csr.2008.03.012.

Nagai, R.H., Ferreira, P.A.L., Mulkherjee, S., Martins, M.V., Figueira, R.C.L., Sousa, S.H.M., Mahiques, M.M., 2014. Hydrodynamic controls on the distribution of surface sediments from the southeast South American continental shelf between 23°S and

38°S. Cont. Shelf Res. 89, 51–60. https://doi.org/10.1016/j.csr.2013.09.016.
Nixon, S.W., 1995. Coastal marine eutrophication – a definition, social causes, and future concerns. Ophelia 41, 199–219.
Odebrecht, C., Djurfeldt, L., 1996. The role of nearshore mixing on phytoplankton size structure of Cape Santa Marta Grande, southern Brazil (Spring 1989). Arch. Fish. Mar. Res. 43 (3), 217–230.
Oksanen, J.F., et al., 2018. Vegan: Community Ecology Package. R Package Version 2.5-2. https://CRAN.R-project.org/package=vegan.
Piola, A.R., Campos, E.J.D., Moller Jr., O.O., Charo, M., Martinez, C.M., 2000. Subtropical shelf front of eastern South America. Geophys. Res. Lett. 105, 6566–6578. https://doi.org/10.1029/1999JC000300.
Piola, A.R., Matano, R.P., Palma, E.D., Moller Jr., O.O., Campos, E.J.D., 2005. The influence of the Plata River discharge on the western South Atlantic shelf. Geophys. Res. Lett. 32, L01603. https://doi.org/10.1029/2004GL021638.
Queiroz, R.L.V., Brandini, F.P., Pellizari, F.M., 2004. Dynamics of microalgal communities in the water-column/sediment interface of the inner shelf off Parana State, southern Brazil. Braz. J. Oceanogr. 52 (3/4), 183–194. https://doi.org/10.1590/S1679-87592004000300002.
R Development Core Team, 2018. R: A Language and Environment for Statistical Computing. R Foundation for Statistical Computing, Vienna, Austria ISBN 3-900051-07-0, URL. http://www.R-project.org.
Redfield, A., Ketchum, B., Richards, F., 1963. The influence of organisms on the composition of sea-water. In: Hill, M.N. (Ed.), The Sea. The Composition of Sea-water Comparative and Descriptive Oceanography, vol. 2. Interscience Publishers, New York, pp. 26–77. https://www.scopus.com/record/display.uri?eid=2-s2.0-0003663268&origin=inward&txGid=2dfb25084f2813f557f81c48cdaed585.
Reynolds, C.S., 2006. The Ecology of Phytoplankton. Cambridge University Press, Cambridge. https://doi.org/10.1017/CBO9780511542145. 535p.
Richardson, K., Beardall, J., Raven, J.A., 1983. Adaptation of unicellular algae to irradiance: an analysis of strategies. New Phytol. 93, 157–191. https://doi.org/10.1111/j.1469-8137.1983.tb03422.x.
Rios, A.F., 1992. El fitoplancton en la Ria de Vigo y sus condiciones ambientales. In: Memoria presentada para optar al grado de Doctora en Biologia por la Universidad de Santiago de Compostela, (192pp. + anexo).
Robertson, L.A., Kuenen, G., 1984. Aerobic denitrification: a controversy revived. Arch. Microbiol. 139, 351–354(https://link.springer.com/article/10.1007/BF00408378).
Sabine, C.L., Feely, R.A., Gruber, N., Key, R.M., Lee, K., Bullister, J.L., ... Millero, F.J., 2004. The oceanic sink for anthropogenic CO_2. Science 305 (5682), 367–371. https://doi.org/10.1126/science.109740.
Savoye, N., Aminot, A., Tréguer, P., Fontugne, M., Naulet, N., Kérouel, R., 2003. Dynamics of particulate organic matter $\delta^{15}N$ and $\delta^{13}C$ during spring phytoplankton blooms in a macrotidal ecosystem (Bay of Seine, France). Mar. Ecol. Prog. Ser. 255, 27–41(http://www.jstor.org/stable/24866946?seq=1#page_scan_tab_contents).
Schlitzer, R., 2018. Ocean Data View. http://odv.awi.de.
SCOR-UNESCO, 1966. Determination of Phtosynthetic Pigments in Sea Water. vol. 1 UNESCO, New York.
Signorini, S.R., McClain, C., 2007. Large-scale forcing impact on biomass variability in the South Atlantic Bight. Geophys. Res. Lett. 34, 1–6. https://doi.org/10.1029/2007GL031121.
Valentin, J.L., 1992. Modelling of vertical distribution of marine primary biomass in the Cabo Frio upwelling region. Ciência e Cultura. Braz. Assoc. Adv. Sci. 44 (2/3), 178–183.
Valiela, I., 2015. Marine Ecological Processes, 2nd ed. Springer-Verlag, New York.
Verity, P.G., Yoder, J.A., Bishop, S.S., Nelson, J.R., Craven, D.B., Blanton, J.O., Roberston, C.Y., Tronzo, C.R., 1993. Composition, productivity and nutrient chemistry of a coastal ocean planktonic food web. Cont. Shelf Res. 13 (7), 741–776.
Vollenweider, R.A., Giovanardi, F.G., Montanari, Ri-Naldi, 1998. Characterization of the trophic conditions of marine coastal waters, with special reference to the NW adriatic Sea: proposal for a trophic scale, turbidity and generalized water quality index. Environmentrics 9, 329–357(http://phytobioimaging.unisalento.it/Portals/7/Documents/TRIX/VollenWeider%20et%20al%201998.pdf).
Wainer, I., Taschetto, A.S., 2006. Climatologia na Região entre o Cabo de São Tomé (RJ) e o Chuí (RS), Diagnóstico para os Períodos Relativos aos Levantamentos Pesqueiros do Programa REVIZEE. In: Rossi-Wongtschowski, C.L.B., Madureira, L.S.-P. (Eds.), O ambiente oceanográfico da plataforma continental e do talude na região Sudeste-Sul do Brasil. Editora da Universidade de São Paulo, São Paulo, pp. 11–120.
Wallner-Kersanach, M., Machado, E.C., 2010. Amostragem e análise de carbono orgânico particulado (COP) e nitrogênio orgânico particulado (NOP). In: MGZ, Baumgarten, Wallner-Kersanach, M., Niencheski LFH (Org.) (Eds.), Manual de Análises em Oceanografia Química, 2nd ed. Editora da FURG, Rio Grande, pp. 156–166.
Yoder, J.A., Atkinson, L.P., Bishop, S.S., Hofmann, E.E., Lee, T.N., 1983. Effect of upwelling on phytoplankton productivity of the outer southeastern United States continental shelf. Cont. Shelf Res. 1, 385–404. https://doi.org/10.1016/0278-4343(83)90004-3.
Yoder, J.A., Atkinson, L.P., Bishop, S.S., Blanton, J.O., Lee, T.N., Pietrafesa, L.J., 1985. Phytoplankton dynamics within Gulf Stream intrusions on the Southeastern United States continental shelf during summer 1981. Cont. Shelf Res. 4, 611–635. https://doi.org/10.1016/0278-4343(85)90033-0.
Zehr, J., Ward, B., 2002. Nitrogen cycling in the ocean: new perspectives on processes and paradigms minireview nitrogen cycling in the ocean: new perspectives on processes and paradigms. Appl. Environ. Microbiol. 68 (3), 1015–1024. https://doi.org/10.1128/AEM.68.3.1015-1024.2002.
Zhang, J., Wu, P., Hao, B., Yu, Z., 2011. Heterotrophic nitrification and aerobic denitrification by the bacterium *Pseudomonas stutzeri* YZN-001. Bioresour. Technol. 102, 9866–9869. https://doi.org/10.1016/j.biortech.2011.07.118.
Zumft, W.G., 1997. Cell biology and molecular basis of denitrification. Microbiology and molecular biology reviews. Am. Soc. Microbiol. 61 (4), 533–616(http://mmbr.asm.org/cgi/reprint/61/4/533?view=long&pmid=9409151).